







Insect eggs trigger systemic acquired resistance against a fungal and an oomycete pathogen

Esteban Alfonso¹, Elia Stahl¹ , Gaétan Glauser² , Etienne Bellani¹, Tom M. Raaymakers³ , Guido Van den Ackerveken³ , Jürgen Zeier⁴  and Philippe Reymond¹ 

¹Department of Plant Molecular Biology, University of Lausanne, Lausanne 1015, Switzerland; ²Neuchâtel Platform of Analytical Chemistry, University of Neuchâtel, Neuchâtel 2000, Switzerland; ³Plant–Microbe Interactions, Department of Biology, Utrecht University, Utrecht 3584 CH, the Netherlands; ⁴Department of Biology, Heinrich Heine University, Universitätsstrasse 1, Düsseldorf D-40225, Germany

Summary

Author for correspondence:
Philippe Reymond
Email: Philippe.Reymond@unil.ch

Received: 21 June 2021
Accepted: 5 September 2021

New Phytologist (2021) 232: 2491–2505
doi: 10.1111/nph.17732

Key words: *Botrytis cinerea*, herbivore interactions, indolic metabolism, insect eggs, *Pieris brassicae*, plant, systemic acquired resistance (SAR).

- Plants are able to detect insect eggs deposited on leaves. In *Arabidopsis*, eggs of the butterfly species *Pieris brassicae* (common name large white) induce plant defenses and activate the salicylic acid (SA) pathway. We previously discovered that oviposition triggers a systemic acquired resistance (SAR) against the bacterial hemibiotroph pathogen *Pseudomonas syringae*.
- Here, we show that insect eggs or treatment with egg extract (EE) induce SAR against the fungal necrotroph *Botrytis cinerea* BMM and the oomycete pathogen *Hyaloperonospora arabidopsidis* Noco2. This response is abolished in *ics1*, *ald1* and *fmo1*, indicating that the SA pathway and the N-hydroxypipicolinic acid (NHP) pathway are involved.
- Establishment of EE-induced SAR in distal leaves potentially involves tryptophan-derived metabolites, including camalexin. Indeed, SAR is abolished in the biosynthesis mutants *cyp79B2*, *cyp79B3*, *cyp71a12*, *cyp71a13* and *pad3-1*, and camalexin is toxic to *B. cinerea in vitro*.
- This study reveals an interesting mechanism by which lepidopteran eggs interfere with plant–pathogen interactions.

Introduction

Plants resist insect herbivory through toxic secondary metabolites, anti-digestive proteins, and emission of volatiles that attract parasitoids. These defenses are generally induced after recognition of herbivore attack, and the resulting transcriptional reprogramming is mainly controlled by the jasmonic acid (JA) pathway (Howe & Jander, 2008; Wu & Baldwin, 2010; Erb & Reymond, 2019). In addition, plants have the ability to detect insect oviposition, even though eggs do not represent a direct threat. Several plant species react to oviposition by activating various direct and indirect defenses (Reymond, 2013; Hilker & Fatouros, 2015). For example, hypersensitive response (HR)-like necrosis, production of reactive oxygen species (ROS), and emission of volatiles that specifically attract egg parasitoids, are efficient ways to inhibit egg survival or development (Hilker *et al.*, 2002; Fatouros *et al.*, 2014; Geuss *et al.*, 2017; Griese *et al.*, 2017, 2021).

In *Arabidopsis*, oviposition induces immune responses that are observed during infection with biotroph pathogens, including localized cell death, ROS and callose production, and expression of hundreds of defense-related genes (Little *et al.*, 2007). Strikingly, the egg-induced transcriptome contains genes regulated by the salicylic acid (SA) signaling pathway (Little *et al.*, 2007; Lortzing, 2020) and oviposition by the butterfly species *Pieris brassicae* (common name large white) triggers SA accumulation

in local and systemic leaves (Bruessow *et al.*, 2010). Also, responses to oviposition or application of crude egg extract (EE) are similar to the recognition of pathogen-associated molecular patterns (PAMPs) during PAMP-triggered immunity (PTI) (Gouhier-Darimont *et al.*, 2013). In support of this finding, phosphatidylcholines (PCs) were recently identified as insect egg-derived immunogenic patterns that trigger PTI (Stahl *et al.*, 2020). In addition, early signaling responses to eggs depend on the receptor-like kinase LecRK-I.8 (Gouhier-Darimont *et al.*, 2013, 2019).

When challenged with a primary infection, plants induce a systemic acquired resistance (SAR) that protects distal parts against a secondary infection by a broad range of pathogens (Sticher *et al.*, 1997; Vlot *et al.*, 2009). We previously discovered that oviposition by *P. brassicae* on *Arabidopsis* induces a SAR against different strains of the bacterial pathogen *Pseudomonas syringae* (Hilfiker *et al.*, 2014). Strikingly, this response was also observed in neighboring plants (Orlovskis & Reymond, 2020). Systemic acquired resistance requires the SA pathway and primes distal leaves for faster and enhanced activation of defenses (Jung *et al.*, 2009; Conrath, 2011; Návarová *et al.*, 2012; Shah & Zeier, 2013). In addition, the lysine catabolite N-hydroxypipicolinic acid (NHP) is a critical regulator of SAR. N-hydroxypipicolinic acid originates from the α -transamination of L-Lys by the aminotransferase AGD2-LIKE DEFENCE RESPONSE PROTEIN1

(ALD1) that generates 2,3-dehydropipecolic acid, which is then reduced to pipecolic acid (Pip) (Ding *et al.*, 2016; Hartmann *et al.*, 2017). Pipecolic acid is further converted to NHP by the N-hydroxylase FLAVIN-DEPENDENT MONOOXYGENASE1 (FMO1) (Chen *et al.*, 2018; Hartmann *et al.*, 2018). It was found that Pip and NHP accumulate in local and systemic leaves after leaf inoculation with *P. syringae* pv *maculicola* (*Psm*), and exogenous treatment with Pip or NHP enhanced immunity to *Psm*. Accordingly, *ald1* and *fmo1* mutants were unable to mount SAR (Návarová *et al.*, 2012; Hartmann *et al.*, 2018). Thus, evidence is accumulating that both the SA and NHP pathways are required for SAR establishment (Hartmann & Zeier, 2019; Zeier, 2021). Interestingly, treatment of Arabidopsis with *P. brassicae* EE triggers SA and Pip accumulation in local and distal leaves, and EE-induced SAR was also shown to depend on the SA and NHP pathways, suggesting a common mechanism between pathogen- and egg-induced SAR (Bruessow *et al.*, 2010; Hilfiker *et al.*, 2014).

Tryptophan-derived, indolic metabolites are important defense molecules in Arabidopsis, and their biosynthesis is activated by a broad spectrum of herbivores and pathogens (Bednarek *et al.*, 2011; Bednarek, 2012; Kettles *et al.*, 2013; Rajniak *et al.*, 2015; Maier *et al.*, 2021). Conversion of tryptophan to indole-3-acetaldoxime is catalyzed by two redundant P450 monooxygenases, CYP79B2 and CYP79B3, from which several branches diverge to generate indole glucosinolates (indole GSs), camalexin, indole-3-carboxylic acid (ICA), and other small indolic molecules (Zhao *et al.*, 2002; Bednarek, 2012). Besides their known role as anti-herbivore compounds (Kim *et al.*, 2008), indole GSs are crucial for resistance against microbial, fungal and oomycete pathogens, primarily as toxic molecules but also as signaling molecules (Bednarek *et al.*, 2009; Clay *et al.*, 2009; Katz *et al.*, 2015). The phytoalexin camalexin accumulates in response to infection by *P. syringae* pv *tomato* DC3000 (*Pst*) and the necrotrophic fungus *Botrytis cinerea* (Tsuji *et al.*, 1992; Kliebenstein *et al.*, 2005), but also in response to oviposition by *P. brassicae* (Valsamakis *et al.*, 2020). Camalexin is synthesized by the cytochrome P450 enzyme PHYTOALEXIN DEFICIENT 3 (PAD3), and the *pad3-1* mutant is highly susceptible to *B. cinerea* (Schuhegger *et al.*, 2006; Ferrari *et al.*, 2007). Indole-3-carboxylic acid accumulates in Arabidopsis leaves infected with *P. syringae*, and its presence in cell walls was correlated with enhanced resistance (Forcat *et al.*, 2010; Stahl *et al.*, 2016). Mutants impaired in ICA conjugates are more susceptible to filamentous pathogens (Pastorczyk *et al.*, 2020). In addition, activation of indolic metabolism is not only restricted to the site of infection. In *P. syringae*-infected Arabidopsis, the accumulation of ICA, indole-3-carbaldehyde and indole-3-ylmethylamine could also be observed in uninfected systemic tissue (Stahl *et al.*, 2016).

Following our discovery that oviposition reduces growth of *Pst* in distal leaves and knowing that SAR is generally effective against a variety of pathogens, we reasoned that egg recognition might trigger a more general defense response. Here, we tested whether egg-induced SAR is efficient against the necrotrophic fungus *B. cinerea* (strain BMM). This plant pathogen has a broad host range and causes grey mold disease, one of the most detrimental fungal diseases in crops (Dean *et al.*, 2012). We show here

that *P. brassicae* oviposition and EE treatment inhibit *B. cinerea* infection in Arabidopsis. Activation of this response is dependent on the SA and NHP pathways and is absent in plants with impaired indolic metabolism. In addition, we found that EE treatment is also efficient against the oomycete *Hyaloperonospora arabidopsidis*, suggesting that oviposition protects plants against a broad range of pathogens.

Materials and Methods

Plant and insect growth conditions

Arabidopsis thaliana (Col-0) plants were grown in potting compost for 4 wk in growth chambers in short day (10 h : 14 h , light : dark) conditions, under 100 $\mu\text{mol m}^{-2} \text{s}^{-1}$ of light, at 20–22°C and 65% relative humidity. For *Hyaloperonospora arabidopsidis* disease assays, Col-0 and *ald1-1* plants were grown on potting soil (mix z2254; Primasta BV, Asten, the Netherlands) at 21°C and 75% relative humidity, under short day conditions. Lines used in this study are described in Supporting Information Methods S1. *Pieris brassicae* was maintained on *Brassica oleracea* var. *gemmifera* in a glasshouse (24°C, 65% relative humidity) (Reymond *et al.*, 2000). *Spodoptera littoralis* eggs were obtained from Syngenta (Stein AG, Switzerland).

Oviposition and treatment with egg extract

For oviposition, 10–15 pots each containing two plants were placed in a 60 × 60 × 60 cm tent containing around 30 *P. brassicae* butterflies. After 24 h, eight plants containing one egg batch on each of two leaves were placed in a growth chamber for 4 d. Before hatching, eggs were gently removed with forceps, and two distal leaves were infected with *Botrytis cinerea*. Control plants were kept in the same conditions without butterflies.

For EE preparation, *P. brassicae* or *S. littoralis* eggs were crushed with a pestle in Eppendorf tubes. After centrifugation (14 000 g for 3 min), the supernatant (EE) was collected and stored at –20°C. For at least 4–6 plants per experiment, 2 × 2 μl of EE were spotted under the surface of each of two leaves. Plants were treated 5 d before *B. cinerea* infection. Untreated plants were used as controls.

For PC application, a PC-mix (purified from chicken egg, 840051; Avanti Polar Lipids, Alabaster, AL, USA) was solved in 1% dimethylsulfoxide (DMSO), 0.5% Glycerol and 0.1% Tween 20 by sonication. On 4–6 plants, 2 × 2 μl of PC (5 $\mu\text{g} \mu\text{l}^{-1}$) were spotted under the surface of each of two leaves. This concentration is found in *P. brassicae* eggs (Stahl *et al.*, 2020). Control plants were treated with 1% DMSO, 0.5% Glycerol and 0.1% Tween 20.

Intra- and interplant SAR experiments were performed according to a previously published protocol (Orlovskis & Reymond, 2020).

Culture of *Botrytis cinerea*, infection and growth assessment

Botrytis cinerea strain BMM (Zimmerli *et al.*, 2001) was grown on 1 × potato dextrose agar (PDA, 39 g l⁻¹; Difco, Chemie

Brunschwig AG, Basel, Switzerland) for 10–14 d in darkness at 20–25°C. Spores were harvested in water and filtered through wool to remove hyphae. Spores were diluted in half-strength potato dextrose broth (PDB, 12 g l⁻¹; Difco) to 5 × 10⁵ spores ml⁻¹ for inoculation. One 5 µl droplet of spore suspension was deposited on the adaxial surface of two leaves per plant. To facilitate spore germination, inoculated plants were kept under a water-sprayed transparent lid to maintain high humidity in a growth chamber under dim light (around 2 µmol m⁻² s⁻¹) during the whole period of infection. After 3 d, lesion size measurements were made using IMAGEJ software v.2.0.0-rc-65/1.51u (<http://imagej.nih.gov/ij>).

To visualize *B. cinerea* structures, inoculated leaves were stained with lactophenol-trypan blue for 2 h at 37°C, cleared in boiling 95% EtOH and stored in 70% EtOH. Observations of *B. cinerea* hyphae were made using a Leica MZ16A stereomicroscope fitted with a DFC310FX camera (Leica Microsystems, Heerbrugg, Switzerland). Images were analyzed with IMAGEJ.

To quantify *B. cinerea* growth, relative expression of *Bc Tubulin* was measured by quantitative polymerase chain reaction (qPCR; for details, see Methods S2).

Determination of antifungal activity

Camalexin (Glaxo Laboratories, Hopkinton, MA, USA) and ICA (Sigma-Aldrich) were dissolved in DMSO. Plugs (diameter 0.5 cm) were taken from a 7-d-old *B. cinerea* culture on 1 × PDA and transferred to six-well plates supplemented with different concentrations of camalexin and ICA in PDA. Control plates contained 0.1% DMSO. For each treatment, radial growth of the fungal colony was measured on two plates ($n = 12$) after 24 h of incubation at 23°C in darkness. Mycelial growth inhibition (MGI) was calculated using the following formula: $MGI \% = ((C - T) / C) \times 100$, where C is the average colony diameter on control plates, and T is the average colony diameter on treated plates.

Infection with *Hyaloperonospora arabidopsidis* and *Pseudomonas syringae*

Infection assays were performed with *H. arabidopsidis* isolate Noco2 (100 spores µl⁻¹). The pathogen was maintained on *Arabidopsis* Col-0 and transferred weekly to fresh 10-d old seedlings. Spores were collected from a *Ws-eds1* mutant to achieve the high level of inoculum used. Two leaves of each tested plant were treated with 2 × 2 µl of EE 1 d before pathogen challenge. Untreated plants were used as controls. The *H. arabidopsidis* spore suspension was applied with a spray gun. Plants were subsequently left to dry to the air for c. 30 min and incubated at 100% humidity at 16°C. Eight days post inoculation, disease severity was determined visually. For spore counts, four systemic leaves from 4–5 EE-treated or control plants were weighed and suspended in 2 ml of water after which the number of spores mg⁻¹ of plant tissue was determined.

Infection with *Pseudomonas syringae* pv *tomato* DC3000 has been described previously (Hilfiker *et al.*, 2014).

Exogenous applications of pipecolic acid

One day before *B. cinerea* infection, 10 ml of a 1 mM D,L-Pip (Sigma-Aldrich) solution was pipetted onto each pot containing one plant. Control plants were supplemented with 10 ml of water.

Salicylic acid quantification and infiltration

Total SA was measured using the bacterial biosensor *Acinetobacter* sp. ADPWH_lux. (Huang *et al.*, 2005, 2006), as described previously (Stahl *et al.*, 2020). For each sample, six leaf discs of 0.7 cm diameter from three plants were pooled and analyzed. For SA infiltration, plant genotypes were infiltrated with 0.25 or 0.5 mM solutions on the abaxial side of two leaves per plant with a 1 ml needleless syringe. H₂O was infiltrated as control. After 4 h, plants were harvested for SA quantification or further infected with *B. cinerea* for 3 d before lesion measurement. For the reporter line PR1::GUS, half of each leaf was infiltrated with 0.5 mM SA, and beta-glucuronidase (GUS) analysis was performed after 4 h (Bruessow *et al.*, 2010).

Metabolite analyses

For each sample, between 10 and 12 leaves (two leaves per plant) were harvested per time point and per treatment. Leaves were then pooled, frozen and ground with a pestle and mortar in liquid nitrogen. Next, 100 mg of frozen leaf powder was placed in a 1.5 ml Eppendorf tube, and 500 µl of extraction buffer (80% methanol, 19.5% water and 0.5% formic acid) was added. After centrifugation (3 min at 14 000 g), 200 µl aliquots were transferred into vials. Camalexin content was measured using ultra-high-performance liquid chromatography coupled to tandem mass spectrometry (UHPLC-MS/MS) (Balmer *et al.*, 2018) and indolic metabolites by quadrupole time-of-flight mass spectrometry (UHPLC-QTOFMS) (Böttcher *et al.*, 2014). Indole-3-carboxylic acid conjugates were quantified as ICA equivalents. The protocol for GS analysis has been described previously (Glauser *et al.*, 2012; for details, see Methods S3).

Insect performance assays

Plants were sprayed with either half-strength PDB or *B. cinerea* spore suspension at a concentration of 5 × 10⁵ spores ml⁻¹. After 48 h, five freshly hatched *P. brassicae* larvae were placed on each of 11 pots, each containing two plants, in a transparent plastic box and kept in a growth chamber during the experiment. Plants were replaced every 3 d by a new set of inoculated plants in order to keep a constant amount of material for feeding larvae. After 6 d of feeding, larvae were weighed on a precision balance (Mettler-Toledo, Greifensee, Switzerland) and placed back on the plants until a final weight measurement after 12 d.

Statistical analyses

Data were analyzed using R software v.3.5.2 (<http://www.R-project.org>). Normal distribution and variance homogeneity of data were evaluated with the Shapiro–Wilk test and Levene's test,

respectively. If not normal, data were log-transformed to enable analyses with parametric tests.

To compare CTL and EE within the same genotype in SAR bioassays, we used a linear mixed model fit by the restricted maximum likelihood (REML) algorithm (package LME4 in R) using plant treatment as a fixed factor and experimental block as a random factor. For multiple comparisons between genotypes, data were analyzed using a linear mixed model with a post-hoc general linear hypothesis test with Tukey contrasts, using plant treatment as a fixed factor and experimental block as a random factor. In both analyses, each block included data from each independent replicate consisting of 8–30 leaves from different plants and from different pots. For feeding bioassays, we used Welch's *t*-test. For metabolite quantifications, we used ANOVA with the Tukey test for post-hoc comparison. Information on sample sizes and summary statistics can be found in Table S1.

Results

Oviposition by *Pieris brassicae* reduces *Botrytis cinerea* infection

Pieris brassicae butterflies were allowed to oviposit on *Arabidopsis* plants, and 4 to 5 d later eggs were gently removed, just before

the hatching of larvae. Two distal leaves were then infected with *B. cinerea* BMM by drop inoculation, and the lesion size was measured after 3 d (Fig. 1a). Compared to control plants, oviposited plants showed a significantly reduced infection (Fig. 1b). As a complementary experiment, plants were pretreated with *P. brassicae* EE. The amount of EE applied onto each plant was equivalent to two egg batches (20–30 eggs per batch). A similar reduction of *B. cinerea* infection was observed on EE-treated plants compared to control plants (Fig. 1c). This result confirms previous observations that EE treatment mimics responses triggered by natural oviposition (Little *et al.*, 2007; Bruessow *et al.*, 2010; Gouhier-Darimont *et al.*, 2019; Orlovskis & Reymond, 2020; Stahl *et al.*, 2020).

Consistent with observations of lesion size, hyphal development was also significantly reduced in distal leaves (Fig. S1). In addition, expression of *B. cinerea* β -tubulin gene was significantly lower in plants pretreated with EE (Fig. S1), providing independent confirmation that EE pretreatment inhibits *B. cinerea* growth. Then, a time-course experiment indicated that inhibition of *B. cinerea* infection can also be observed in local leaves pretreated with EE from 2 to 3 d after infection, and that this protection reaches distal leaves only after 3 d (Fig. S2).

To explore the generality of egg-derived inhibition of *B. cinerea* infection, we treated plants with EE from the generalist

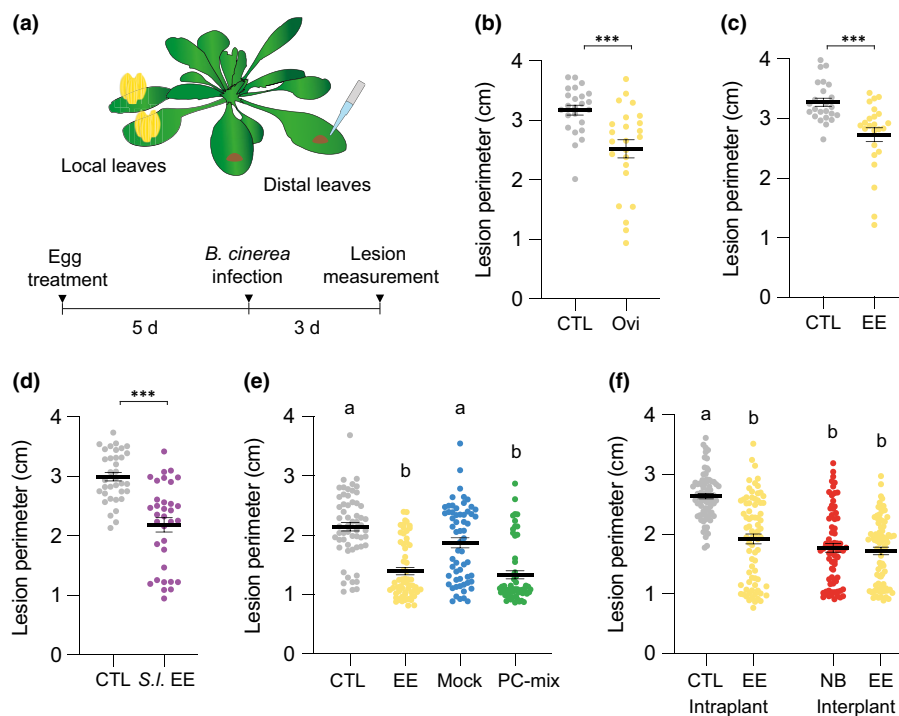


Fig. 1 Oviposition and treatment with egg extract (EE) reduce *Botrytis cinerea* BMM infection. (a) Experimental design. (b–d) Effect of 5 d-pretreatment with *Pieris brassicae* oviposition (Ovi) (b), *P. brassicae* EE (c), or *Spodoptera littoralis* EE (d) on *B. cinerea* growth. Lesion perimeter in distal leaves was measured 3 d after inoculation. Inoculated plants without pretreatment were used as controls (CTL). (e) Plants were pretreated with either *P. brassicae* EE or a $5 \mu\text{g} \mu\text{l}^{-1}$ solution of phosphatidylcholine (PC)-mix from chicken egg. Respective controls consisted of CTL plants or plants treated with a mock solution (Mock). (f) Egg extract pretreatment reduced *B. cinerea* growth in distal leaves when compared to CTL plants grown separately (intraplant systemic acquired resistance (SAR)). No difference in *B. cinerea* growth was observed when EE-treated and untreated neighbor plants (NB) were in the same pot (interplant SAR). Means \pm SE of three independent experiments are shown ($n = 8–30$ per experiment). Significant differences between control and treated plants are indicated (linear mixed model; ***, $P < 0.001$). Lowercase letters indicate significant difference at $P < 0.05$ (linear mixed model and post-hoc general linear hypothesis test with Tukey contrasts). Dots indicate individual values.

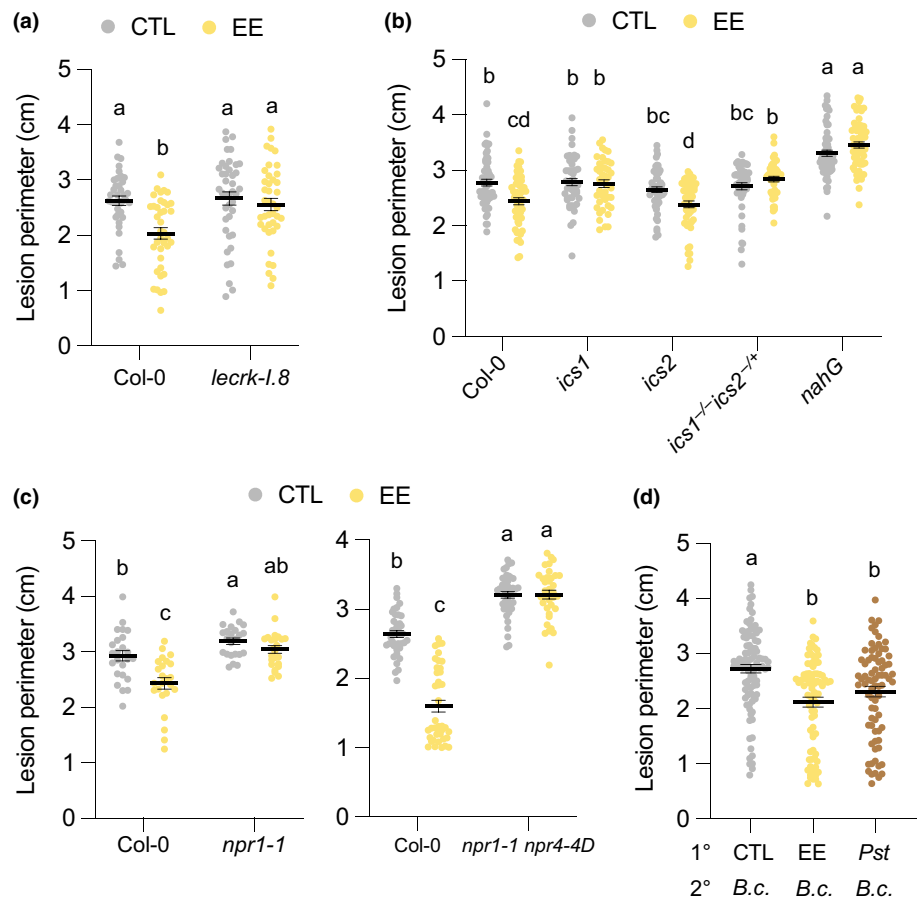


Fig. 2 Egg extract-induced systemic acquired resistance depends on the salicylic acid pathway. (a–c) Plant genotypes were pretreated with *Pieris brassicae* egg extract (EE) for 5 d and further infected with *Botrytis cinerea* BMM for 3 d. Lesion perimeter was measured in control (CTL) and distal leaves from EE-treated plants (EE). The double mutant *ics1 ics2* was homozygous for *ics1* ($^{-/-}$) and heterozygous for *ics2* ($^{-/+}$). (d) Local leaves (1°) were untreated (CTL), treated with EE for 5 d (EE) or infiltrated with *Pseudomonas syringae* pv *tomato* DC3000 (*Pst*) for 2 d. Distal leaves (2°) were then inoculated with *B. cinerea* spore suspension (*B.c.*) for 3 d before lesion perimeter measurement. Means \pm SE of three independent experiments are shown ($n = 8$ –28 per experiment). Lowercase letters indicate significant difference at $P < 0.05$ (linear mixed model and post-hoc general linear hypothesis test with Tukey contrasts). Dots indicate individual values.

herbivore *Spodoptera littoralis*. Like with *P. brassicae* EE, pretreatment with *S. littoralis* EE significantly reduced fungal infection (Fig. 1d). Pretreatment with a solution of phosphatidylcholines (PC-mix), known to contain bioactive PCs found in *P. brassicae* eggs (Stahl *et al.*, 2020), inhibited *B. cinerea* infection to the same extent as EE, indicating that egg-induced SAR is triggered following perception of an egg-associated molecular pattern (Fig. 1e).

We previously found that egg-induced SAR against *P. syringae* extends to neighboring plants through an as-yet unknown root-mediated signal (Orlovskis & Reymond, 2020). Strikingly, inhibition of *B. cinerea* growth after EE pretreatment was also observed in untreated plants that were grown in the same pot (Fig. 1f). Thus, EE pretreatment of focal plants activates resistance in neighbors against different pathogens. Future investigations might reveal whether the same signal is used for both responses and whether this phenomenon operates between different species.

Egg extract-induced systemic acquired resistance against *Botrytis cinerea* requires salicylic acid and N-hydroxypipicolinic acid signaling

Signaling of Arabidopsis responses to *P. brassicae* oviposition involves early LecRK-I.8 activity followed by triggering of the SA pathway (Gouhier-Darimont *et al.*, 2013, 2019; Stahl *et al.*, 2020). In the *lecrk-I.8*T-DNA knockout mutant, infection by *B. cinerea* was similar to that observed in Col-0. However, EE

pretreatment did not trigger SAR in the mutant, indicating that LecRK-I.8 contributes to the triggering of SAR but not to basal resistance against this fungus (Fig. 2a).

Salicylic acid biosynthesis requires primarily the activity of ISOCHORISMATE SYNTHASE 1 (ICS1), with a limited contribution of its homolog ICS2 (Garcion *et al.*, 2008). Egg extract-induced SAR was absent in *ics1* (*sid2-1* allele (Nawrath & Métraux, 1999)) and in the semi-homozygous *ics1^{-/-} ics2^{-/+}*, whereas it was conserved in *ics2*, demonstrating the crucial role of ICS1 in this response (Fig. 2b). Also, SAR was lost in the SA-degrading transgenic line *nahG* (Fig. 2b). In line with the SAR phenotype, EE treatment induced strong SA accumulation in Col-0 and *ics2*, while levels were undetectable in *ics1*, *ics1^{-/-} ics2^{-/+}*, and *nahG* (Fig. S3). Although we could not test a fully homozygous *ics1 ics2* double mutant, which shows severely impaired growth (Garcion *et al.*, 2008), our data indicate that ICS1-dependent SA accumulation is required for the systemic induction of defense by EE treatment, with no apparent contribution of ICS2.

In PTI signaling, NON EXPRESSOR OF *PR* GENES1 (NPR1) and NPR3/NPR4 are important downstream modulators of defense gene expression (Zhou & Zhang, 2020). They all bind SA, but NPR1 acts as a positive activator of transcription, whereas NPR3 and NPR4 are repressors (Zhou & Zhang, 2020). We previously found that EE-induced *PR1* expression was significantly reduced in *npr1-1* (Gouhier-Darimont *et al.*, 2013). Here,

EE treatment did not significantly reduce *B. cinerea* growth in *npr1-1*, although there was a trend for a weak response in the mutant (Fig. 2c). A residual signaling activity in *npr1-1* is postulated to be due to the inhibition of NPR3/NPR4 repressor activity by SA (Liu *et al.*, 2020). Indeed, using the *npr1-1 npr4-4D* double mutant, which includes the gain-of-function mutant *npr4-4D* and is blocked in SA signaling (Liu *et al.*, 2020), we could not detect any SAR (Fig. 2c). The double mutant and *npr1-1* were also significantly more susceptible to *B. cinerea* in the absence of EE pretreatment. Thus, these findings demonstrate a contribution of SA signalling to basal resistance and EE-induced SAR against *B. cinerea*.

Collectively, our data suggest that activation of PTI signaling by insect eggs generates SAR against *B. cinerea* BMM. To test whether this is similar to a bacterial-induced SAR, we infiltrated primary leaves with *Pst* for 2 d before infecting distal leaves with *B. cinerea*. Strikingly, EE or *Pst* pretreatment led to a similar inhibition of fungal growth compared to untreated controls (Fig. 2d).

The NHP pathway is central for bacterial-induced SAR and is required for the establishment of primed defenses in systemic leaves (Hartmann & Zeier, 2019; Zeier, 2021). We have previously shown that this pathway is also necessary for egg-induced SAR against bacterial pathogens (Hilfiker *et al.*, 2014). Here, we used the Pip biosynthesis mutant *ald1* and the *fmo1* mutant impaired in Pip conversion to NHP. Upon secondary *B. cinerea* infection, both mutants showed a lack of EE-induced SAR, indicating that the NHP pathway is required for systemic inhibition of fungal growth (Fig. 3a). To further assess the role of Pip in EE-induced SAR, we exogenously applied 1 mM Pip solution to the soil 1 d before *B. cinerea* inoculation. In Col-0, Pip application alone did not inhibit *B. cinerea* growth and did not enhance EE-induced SAR (Fig. 3b). This suggests that Pip is not sufficient to activate SAR in the absence of an EE-derived stimulus. However, Pip application to *ald1* was able to restore SAR after EE treatment, indicating that Pip can complement the biosynthesis mutant and acts downstream of an EE stimulus. Finally, Pip application had no effect on *fmo1*, which did not display EE-induced SAR in any condition, confirming the need for hydroxylation of Pip by FMO1 to generate the active SAR signal NHP (Fig. 3b).

We next reasoned that the combined accumulation of SA and NHP may be sufficient to generate SAR. We first established that leaf SA infiltration was able to induce *PR1* expression using a *PR1::GUS* reporter plant (Fig. S4a) and that infiltration of 0.25 mM SA in Col-0 yielded the same amounts that accumulate after 5 d of EE treatment (Fig. S4b). However, treatment with SA alone or in combination with Pip was not able to inhibit *B. cinerea* growth in Col-0, *ald1* or *fmo1*, suggesting that induction of SAR by EE requires additional components.

Camalexin is involved in egg extract-induced systemic acquired resistance

Given the reported role of indolic metabolism in plant immunity, we asked whether any indolic biosynthetic branch is responsible for the inhibition of *B. cinerea* infection. The *cyp79b2 cyp79b3* double mutant is blocked in tryptophan conversion to

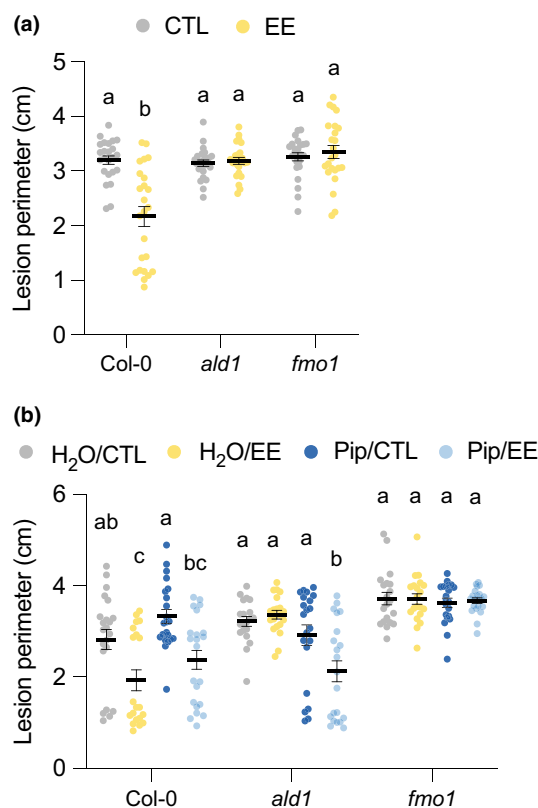


Fig. 3 Egg extract (EE)-induced systemic acquired resistance depends on the N-hydroxy-pipecolic acid pathway. (a) Plant genotypes were pretreated with *Pieris brassicae* EE for 5 d and further infected with *Botrytis cinerea* BMM for 3 d. Lesion perimeter was measured in control (CTL) and distal leaves from EE-treated plants (EE). Means \pm SE of three independent experiments are shown ($n = 8$ per experiment). Lowercase letters indicate significant difference at $P < 0.05$ (linear mixed model and post-hoc general linear hypothesis test with Tukey contrasts). (b) Plant genotypes were pretreated with *P. brassicae* EE for 5 d and further infected with *B. cinerea*. H₂O or 1 mM pipecolic acid (Pip) was applied to the soil 1 d before infection, and lesion perimeter measurements were recorded 3 d after infection. Means \pm SE of three independent experiments are shown ($n = 6-8$ per experiment). For each genotype, different lowercase letters indicate significant differences at $P < 0.05$ (ANOVA followed by Tukey's Honest Significant Difference test). Dots indicate individual values.

indole-3-acetaldoxime (IAOx), a central molecule from which several indolics derive, including indole GSs, 4-hydroxyindole-3-carbonyl nitrile (4-OH-ICN), camalexin, and ICA (Böttcher *et al.*, 2014; Rajniak *et al.*, 2015) (Fig. 4a). Strikingly, EE-induced SAR was abolished in *cyp79b2 cyp79b3* (Fig. 4b). In addition, the mutant was significantly more susceptible to *B. cinerea* infection in the absence of EE pretreatment, indicating that tryptophan-derived compounds are important for both basal resistance and SAR.

Indole GSs contribute to Arabidopsis immunity against bacterial and fungal pathogens, including *B. cinerea* (Bednarek *et al.*, 2009; Clay *et al.*, 2009; Xu *et al.*, 2016). MYB34, MYB51, and MYB122 transcription factors regulate the biosynthesis of indole GSs, but also of camalexin and other Trp-derived metabolites (Frerigmann & Gigolashvili, 2014; Frerigmann *et al.*, 2016). The *myb34 myb51 myb122* (*tmyb*) triple mutant lacks indole

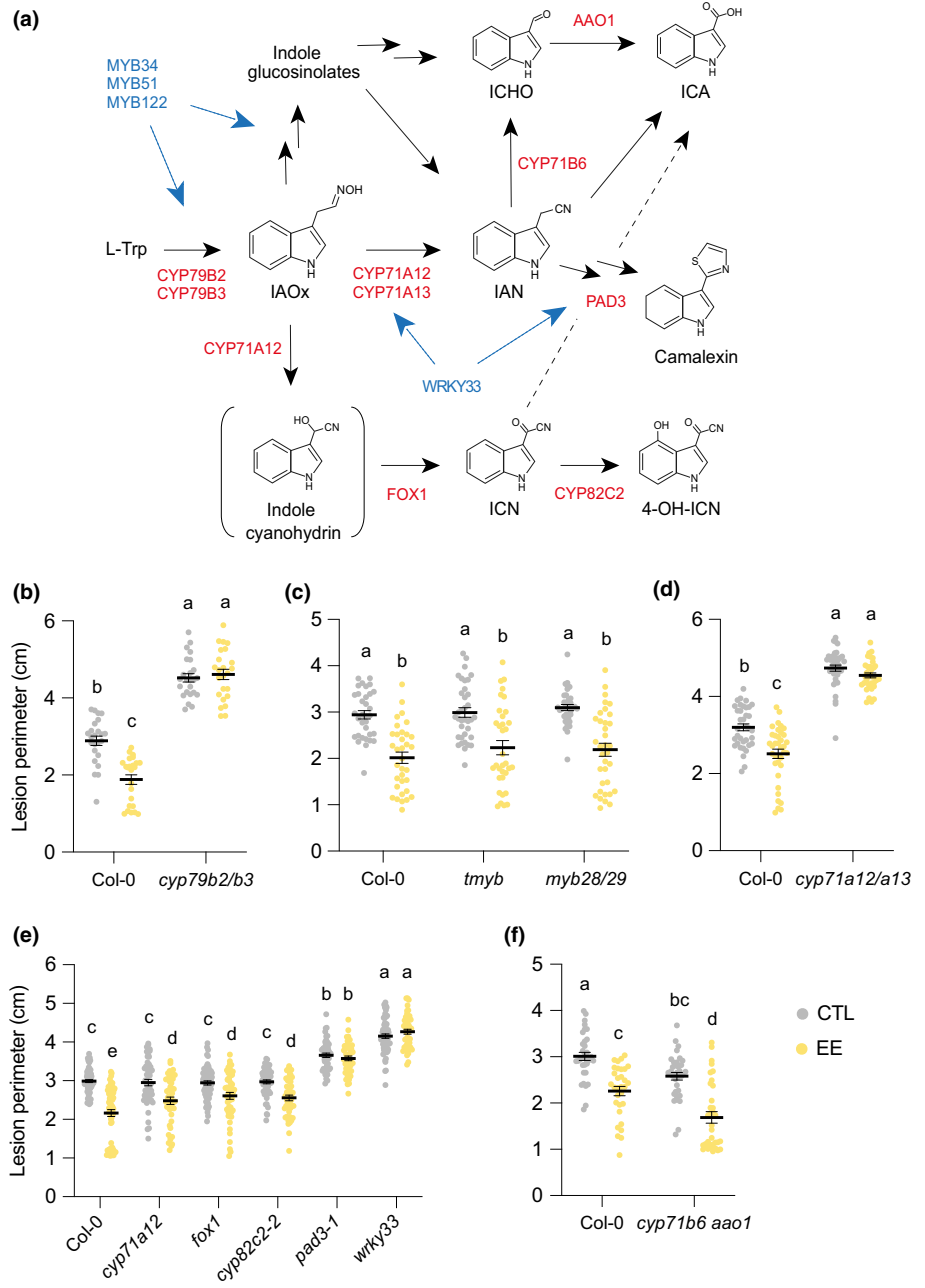


Fig. 4 Establishment of egg extract (EE)-induced systemic acquired resistance requires tryptophan-derived compounds. (a) Simplified scheme of biosynthesis of tryptophan derivatives and position of biosynthesis (red) and regulatory (blue) genes tested in this study. Brackets indicate an unstable intermediate. Several arrows indicate multiple steps. 4-OH-ICN, 4-hydroxy-ICN; IAN, indole-3-acetonitrile; IAOx, indole-3-acetaldoxime; ICA, indole-3-carboxylic acid; ICHO, indole-3-carbaldehyde; ICN, indole carbonyl nitrile; L-Trp, tryptophan. (b–f) Plant genotypes were pretreated with *Pieris brassicae* EE for 5 d and further infected with *Botrytis cinerea* BMM for 3 d. Lesion perimeter was measured in control (CTL) and distal leaves from EE-treated plants (EE). Means \pm SE of three independent experiments are shown ($n = 8–21$ per experiment). Lowercase letters indicate significant difference at $P < 0.05$ (linear mixed model and post-hoc general linear hypothesis test with Tukey contrasts). Dots indicate individual values. The ‘*tmyb*’ label on the x-axis in part (c) represents *myb34 myb51 myb122*.

GSs, but not aliphatic GSs (Frerigmann & Gigolashvili, 2014). However, EE-induced inhibition of *B. cinerea* growth was similar in Col-0 and in the indole GS mutant (Fig. 4c). In addition, a *myb28 myb29* double mutant lacking aliphatic GSs (Beekwilder *et al.*, 2008) displayed EE-induced SAR, suggesting that neither GS type is involved in the inhibition of *B. cinerea* BMM growth (Fig. 4c). Next, whole-leaf concentrations of both GS classes were not significantly different between treated and control plants over a time-course of 12 h to 48 h after inoculation, indicating that neither EE nor *B. cinerea* induced GS accumulation (Fig. S5a,c; Table S2). In addition, we confirmed that *tmyb* lacks indole GSs, even after EE or *B. cinerea* treatment, but has wild-type levels of aliphatic GSs (Fig. S5b,d; Table S3).

In leaves, oxidation of IAOx by CYP71A12 and CYP71A13 generates IAN, which is the common precursor of 4-OH-ICN, ICA, and camalexin (Fig. 4a). Egg extract-induced SAR was abolished in the *cyp71a12 cyp71a13* double mutant, suggesting the involvement of one or several of these metabolites (Fig. 4d). To assess the specific role of 4-OH-ICN, which exhibits antimicrobial activity (Rajniak *et al.*, 2015), we used mutants in three consecutive biosynthetic steps. We observed a significant EE-induced SAR in *cyp71a12*, *fox1*, and *cyp82c2-2*, thus eliminating 4-OH-ICN as a player in EE-induced SAR against *B. cinerea* BMM (Fig. 4e).

Several pathways can lead to ICA formation, from degradation of indole GSs, conversion of IAN, and hydrolysis of ICN

(Fig. 4a). Some steps involve the activity of CYP71B6 and/or AAO1. Egg extract-induced SAR was similar in Col-0 and the *cyp71b6 aao1* double mutant (Fig. 4f). However, ICA analysis revealed that this metabolite accumulated strongly after *B. cinerea* infection, with or without EE pretreatment, and that concentrations were similar in Col-0 and *cyp71b6 aao1* (Fig. S6). Also, ICA conjugates were induced by EE treatment but not by *B. cinerea*, though the concentrations were similar between Col-0 and *cyp71b6 aao1* (Fig. S7). This finding suggests another route for ICA accumulation during *B. cinerea* infection or EE treatment, similar to what was recently reported for the necrotroph *Plectosphaerella cucumerina* (Pastorczyk *et al.*, 2020). However, ICA and ICA conjugate accumulation was also unaffected in *cyp71a12 cyp71a13*, although this mutant displayed no EE-induced SAR (Fig. S6 and S7). This finding indicates that IAN is not a precursor for ICAs in these conditions and that the impaired SAR in this mutant cannot be attributed to a lack of ICAs.

Finally, SAR was abolished in *pad3-1*, a mutant of CYP71B15 that catalyzes the last step in camalexin biosynthesis (Schuhegger *et al.*, 2006) and forms a core metabolon with CYP71A12/A13 and CYP79B2 (Mucha *et al.*, 2019). Consistently, SAR was also absent in *wrky33*, a mutant of the transcription factor WRKY33 that regulates the expression of camalexin biosynthesis genes (Birkenbihl *et al.*, 2012; Liu *et al.*, 2015; Zhou *et al.*, 2020) (Fig. 4e). Also, both mutants displayed significantly enhanced basal susceptibility to *B. cinerea* compared to Col-0. Thus, these data point to camalexin as a key component of EE-induced SAR against *B. cinerea* BMM.

Camalexin accumulation

The finding that EE-induced SAR was lost in mutants impaired in camalexin biosynthesis led us to quantify this metabolite in response to EE treatment and/or *B. cinerea* infection. First, EE treatment triggered a strong accumulation of camalexin, but this was only observed in local leaves (Fig. S8). This finding could explain the reduced *B. cinerea* growth in local leaves after EE treatment (Fig. S2). Then, *B. cinerea* infection produced a significant increase in camalexin from 12 h to 48 h after inoculation; however, this increase was similar when local leaves were pretreated with EE (Fig. 5a,b). In addition, the camalexin accumulation found in both *ald1* and *ics1* was similar to that observed in Col-0, irrespective of EE pretreatment (Fig. 5a,b). These data suggest that the SA and NHP pathways are crucial to generate the SAR signal but not for *B. cinerea*-induced camalexin production. Further analysis of camalexin concentrations every 3 h between 12 and 24 h after *B. cinerea* infection did not reveal an earlier or enhanced accumulation of this metabolite.

Camalexin secretion to the leaf surface is crucial for defense against *B. cinerea* in Arabidopsis (Khare *et al.*, 2017; He *et al.*, 2019). To test if EE pretreatment might prime camalexin secretion after *B. cinerea* infection, we incubated infected leaves for 30 s in 80% MeOH and measured camalexin concentrations in the solution. However, surface camalexin concentrations were similar in CTL or EE-treated Col-0 plants from 12 to 24 h after infection, and the same was true for *ald1* plants (Fig. S9).

Camalexin has known antifungal properties against *B. cinerea* (Ferrari *et al.*, 2003; Kliebenstein *et al.*, 2005). In addition, ICA is toxic to diverse plant fungal pathogens *in vitro* (Kavitha *et al.*, 2010; Pedras & Hossain, 2011). To test the antifungal role of these indolics against the strain used in this study, we monitored *B. cinerea* BMM growth *in vitro* on plates supplemented with increasing concentrations. Camalexin showed a steep dose-dependent effect on fungal growth, reaching >90% of inhibition between 20 and 50 $\mu\text{g ml}^{-1}$. This inhibition was similar to that observed previously for sensitive *B. cinerea* strains DGUS-1 and GLUK-1 (Kliebenstein *et al.*, 2005). Interestingly, ICA also inhibited *B. cinerea* growth, although with a weaker activity (37% inhibition at 50 $\mu\text{g ml}^{-1}$) (Fig. 5c).

To ensure that the conserved EE-induced SAR that was observed in different indolic mutants was not due to a compensatory overaccumulation of camalexin, we quantified this compound in response to EE treatment and/or *B. cinerea* infection. However, camalexin concentrations were not different from Col-0 in *cyp71a12* or *cyp71b6 aao1*. On the contrary, camalexin was undetectable in *cyp71a12 cyp71a13* and *pad3-1*, which is consistent with their impaired EE-induced SAR (Fig. S10). In addition, *B. cinerea* infection triggered similar ICA accumulation in Col-0 and *pad3-1*, strongly suggesting that the absence of EE-induced SAR in this mutant is specifically due to the lack of camalexin (Fig. S6).

Besides their role in regulating indole GS biosynthesis, MYB34, MYB51, and MYB122 have also been shown to differentially regulate the accumulation of camalexin and ICA in response to UV, flagellin or *P. cucumerina* treatments (Frerigmann *et al.*, 2015, 2016). However, both indolic metabolites accumulated similarly in Col-0 and *tmyb* after *B. cinerea* infection, indicating that the contribution of these MYBs to different branches of the Trp pathway depends on the (a)biotic conditions considered (Figs S6, S10).

Reduced performance of *Pieris brassicae* larvae on *Botrytis cinerea*-infected plants

Whole-plant reduction of *B. cinerea* infection by insect egg pretreatment may benefit hatching larvae. To test the effect of *B. cinerea* on *P. brassicae* larvae, we measured insect performance on infected plants. After 12 d, larvae were significantly smaller when feeding on infected plants compared to plants sprayed with PDB only (Fig. 6).

Egg extract-induced systemic acquired resistance against *Hyaloperonospora arabidopsidis*

To test whether EE-induced SAR can target other plant pathogens, we monitored infection of the oomycete *Hyaloperonospora arabidopsidis* Noco2 (*Hpa*), which is an obligate biotroph that causes downy mildew on Arabidopsis (Coates & Beynon, 2010). Egg extract pretreatment strongly enhanced resistance against *Hpa*. Remarkably, <10% of systemic leaves from EE-treated plants showed symptoms of infection, whereas >90% of control plants were infected. By contrast, *ald1* plants were fully infected in the presence or absence of EE pretreatment (Fig. 7a).

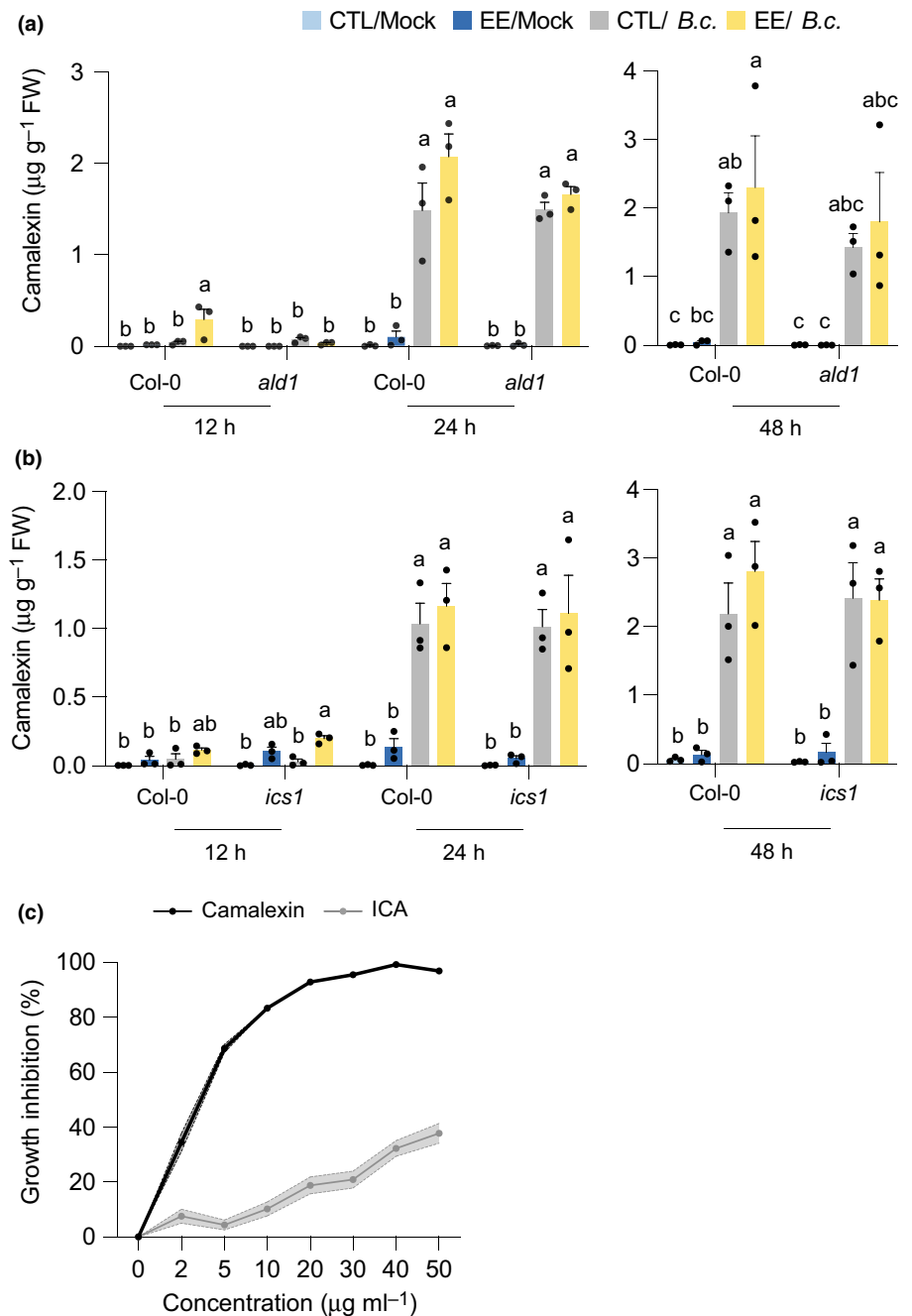


Fig. 5 Camalexin accumulation after egg extract and *Botrytis cinerea* BMM treatment. Plant genotypes were pretreated with *Pieris brassicae* egg extract (EE) for 5 d, and distal leaves were further treated with a mock solution or infected with *B. cinerea*. Untreated plants were used as controls (CTL). (a,b) Camalexin concentrations were measured in distal leaves. Means \pm SE of three independent experiments are shown ($n = 10$ – 12 per experiment). For each time point, different letters indicate significant differences at $P < 0.05$ (ANOVA followed by Tukey's Honest Significant Difference test). (c) *In vitro* growth inhibition assay. Radial growth of a *B. cinerea* colony growing on potato dextrose agar plates supplemented with different concentrations of camalexin or indole-3-carboxylic acid (ICA) was measured after 24 h of incubation. Solid line, mean; shaded band, SE ($n = 12$). This experiment was repeated twice with similar results.

Similarly, the spore number on systemic leaves of EE-treated plants was drastically reduced in Col-0, whereas this effect was much less pronounced in *ald1* (Fig. 7b). These results illustrate a wide-ranging protective effect of EE treatment and the important role of the NHP pathway in this response. This finding also supports the observation that exogenous application of Pip or NHP confers resistance to *Hpa* in Arabidopsis (Hartmann *et al.*, 2018).

Discussion

Our data show that activation of the SA pathway in response to oviposition leads to a systemic enhanced protection against a

necrotrophic fungus. This finding is somewhat surprising given that plant resistance to necrotrophs is generally known to require JA/ethylene (ET) pathways (Pieterse *et al.*, 2012). There are, however, reports pointing to a contribution of SA signaling in defense against *B. cinerea*. Exogenous SA application decreased *B. cinerea* lesion size, and the *ein2-1 npr1-1* double mutant was more susceptible than the single ET mutant *ein2-1* (Ferrari *et al.*, 2003). Enhanced basal susceptibility of *ics1* (*sid2-1*) and *npr1-1* to *B. cinerea* was reported (Nie *et al.*, 2017). Also, phenotypic and transcriptomic analyses of Arabidopsis plants infected with *B. cinerea* isolates support a more intricate role of the JA and SA pathways in resistance (Zhang *et al.*, 2017). There is also growing evidence that the trophic

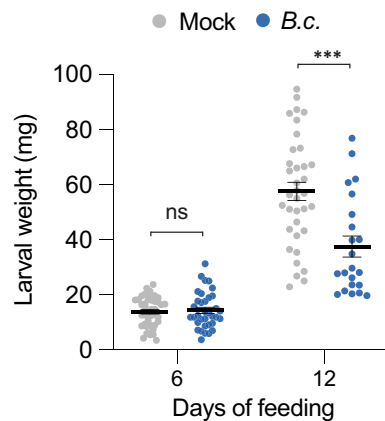


Fig. 6 *Pieris brassicae* larval development is inhibited in *Botrytis cinerea* BMM-infected plants. Plants were sprayed with a suspension of *B. cinerea* spores (*B.c.*) or mock solution (control; CTL). Freshly hatched *P. brassicae* were then placed on plants for a total of 12 d. Newly infected plants were placed every 3 d, in order to have sufficient material for the larvae to feed on. Larval weight was recorded after 6 and 12 d. Means \pm SE are shown ($n = 22$ –43). Significant differences between control and infected plants are indicated (Welch's two sample *t*-test; ***, $P < 0.001$; ns, not significant). This experiment was repeated twice with similar results. Dots indicate individual values.

lifestyle of *B. cinerea* is more plastic than previously thought (van Kan *et al.*, 2014; Veloso & van Kan, 2018), and this may explain why the SA pathway may contribute in part to defense against this fungus. In line with these findings, we show here that *nabG*, *npr1-1* and *npr1-1 npr4-4D*, which are SA signaling null mutants, have elevated basal susceptibility to *B. cinerea* BMM.

Interestingly, oviposition was also shown to enhance defenses against chewing larvae, a resistance that normally requires the JA pathway (Lortzing *et al.*, 2019, 2020; Valsamakis *et al.*, 2020). In addition, *P. brassicae* eggs trigger the accumulation of JA and JA-Ile in *Arabidopsis* (Valsamakis *et al.*, 2020). The reported specificity and antagonism of the SA/JA pathways (Pieterse *et al.*, 2012) may thus not be as strict as anticipated and may depend on the plant–biotic interaction considered.

We also demonstrate that EE-induced SAR against *B. cinerea* BMM and *H. arabidopsidis* Noco2 requires the NHP pathway, consistent with our previous finding with EE-induced SAR against *Pst* and *Psm* (Hilfiker *et al.*, 2014). There is thus apparently a shared mechanism for SAR activation in response to insect eggs and bacteria, which both trigger SA and NHP pathways. In line with this hypothesis, we found that *Pst* infection of local leaves triggers SAR against *B. cinerea*. It would be interesting to test whether any biotic stress that leads to SA accumulation generates a similar NHP-dependent SAR or whether additional specific cues from the attacker are necessary. Noticeably, we found that Pip complementation of *ald1* was not sufficient to restore SAR against *B. cinerea* but that EE pretreatment was necessary, implying an additional egg-derived signal. Also, we could not induce SAR by co-treatment with Pip and SA, indicating that more components are needed. Alternatively, SA infiltration might have been unable to replace the natural EE-induced SA accumulation and generation of a SAR signal. By contrast, Pip complementation of *ald1* was sufficient to restore SAR against

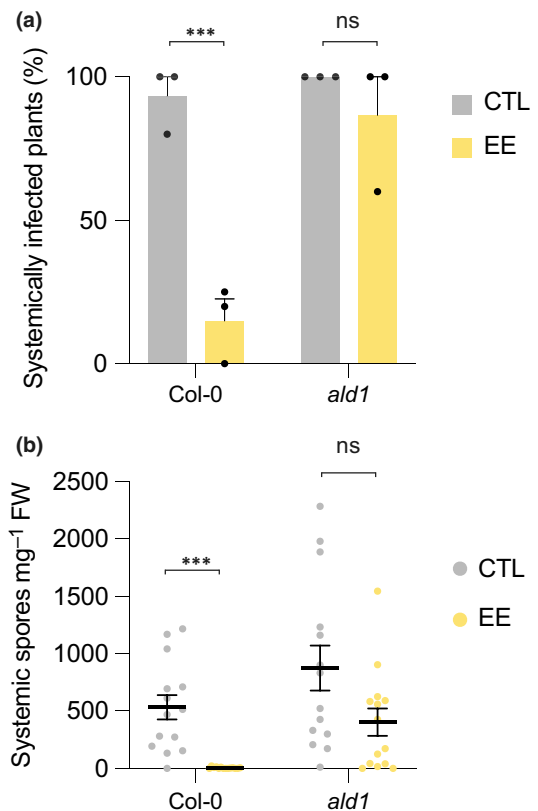


Fig. 7 Egg extract-induced systemic acquired resistance reduces *Hyaloperonospora arabidopsidis* Noco2 infection. Effect of 1 d-pretreatment with *Pieris brassicae* egg extract (EE) on *H. arabidopsidis* infection in distal leaves was measured 8 d after inoculation. Inoculated plants without pretreatment were used as controls. Percentage of systemically infected plants (a) or number of spores on systemic leaves (b) were quantitated. Mean values \pm SE of three independent experiments are shown ($n = 4$ –5 per experiment). Significant differences between control and treated plants are indicated ((a) Pearson's chi-squared test; (b) Welch's two sample *t*-test; ***, $P < 0.001$; ns, not significant).

Psm (Návarová *et al.*, 2012). More work will be needed to investigate what distinguishes bacteria- from egg-induced SAR at the molecular level, but results from previous work and this study indicate that both phenomena depend on the SA and NHP pathways (Hartmann & Zeier, 2019; Zeier, 2021).

We identified camalexin as a crucial indolic compound potentially associated with the execution of EE-induced SAR against a sensitive *B. cinerea* strain. Indeed, EE-induced SAR is abolished in *Arabidopsis* mutants that are blocked in camalexin accumulation but not in mutants impaired in the biosynthesis of other Trp-derived metabolites, like indole GS or 4-OH-ICN. We also show that camalexin is toxic to the *B. cinerea* BMM strain used in this study. Interestingly, bacteria-induced SAR against *P. syringae* developed in hydroponically cultivated *cyp79b2 cyp79b3* (Stahl *et al.*, 2016), indicating a dispensable function of tryptophan-derived compounds for SAR towards bacterial challenge. This finding points to a difference in the establishment of SAR between bacterial and fungal pathogens. In support of this hypothesis, camalexin has been shown not to protect plants against bacterial pathogens (Bednarek, 2012).

While we present genetic evidence for a role of camalexin in EE-induced SAR against the BMM strain, measurements of camalexin accumulation in the infected leaf, and specifically at the leaf surface, could not reveal a difference between control and EE-pretreated plants. In addition, although *ald1* and *ics1* mutants are impaired in the generation of a SAR signal, they displayed similar camalexin concentrations to Col-0 after *B. cinerea* infection. For instance, *B. cinerea* is known to rapidly detoxify camalexin into IAN and ICA (Pedras *et al.*, 2011). As our *in vitro* toxicity assay showed that ICA is significantly less antifungal than camalexin, one hypothesis could be that EE pretreatment inhibits camalexin detoxification by *B. cinerea*. Alternatively, camalexin may be metabolized *in planta* to an as-yet unknown potent antifungal compound, and this conversion would be enhanced by SAR signal(s). Also, EE-induced SAR may potentiate the toxicity of camalexin towards *B. cinerea*. An alternative explanation could be that the higher basal susceptibility of mutants that lack camalexin cannot be overcome by the egg-induced SA/NHP-dependent SAR, which may operate via a distinct mechanism. Clearly, further research will be needed to elucidate the molecular steps that connect egg-triggered SA/NHP pathways to the inhibition of *B. cinerea* BMM, whether this is through indolic metabolism or through other defensive compounds.

There are number of *B. cinerea* strains that are resistant or less sensitive to camalexin, for instance through transporter-mediated efflux (Kliebenstein *et al.*, 2005; Stefanato *et al.*, 2009). Whether EE-induced SAR is efficient against these strains, and through which mechanism/metabolite, are important questions that deserve future investigation.

We showed that concentrations of indole GSs are not affected by EE treatment nor by *B. cinerea* BMM infection. Given that we sampled whole leaves, however, we cannot exclude the possibility that more specific changes occurred at a finer scale. Indeed, previous work has shown higher indole and aliphatic GS concentrations at increasing distance from the *B. cinerea* lesion, and this could be modulated by EE pretreatment (Kliebenstein *et al.*, 2005). However, the finding that *tmyb* and *myb28 myb29* are still able to develop a normal EE-induced SAR against the BMM strain strongly suggests that GSs do not play a role in this phenomenon. Although this *tmyb* lacks indole GSs (Frerigmann & Gigolashvili, 2014), it is also impaired in the UV-induced conversion of IAOx to several indolic metabolites, including camalexin and ICA, albeit not in response to infection with *P. cucumerina* (Frerigmann *et al.*, 2016). We also found that *tmyb* has wild-type camalexin and ICA levels after *B. cinerea* infection, further supporting the role of camalexin in EE-induced SAR. Interestingly, PEN2-dependent metabolism of indole GS has been reported to be important for innate immunity against bacterial and fungal pathogens, and is connected to the SA pathway (Bednarek *et al.*, 2009; Clay *et al.*, 2009; Bednarek, 2012). However, conservation of EE-induced SAR in *tmyb* makes it unlikely that indole GS derivatives play a signaling role in the response against the BMM strain.

Our observation that GS mutants and Col-0 have a similar basal resistance to the BMM strain differs from the findings of other studies indicating that aliphatic and/or indole GSs are involved in basal resistance to certain *B. cinerea* strains (Buxdorf

et al., 2013). Similarly, the *cyp82c2* mutant displayed increased susceptibility to *B. cinerea* in other studies, suggesting an important role for 4-OH-ICN (Rajniak *et al.*, 2015; Liu *et al.*, 2020). Thus, the role of GS and 4-OH-ICN in EE-induced SAR may also depend on the strain considered and should be explored further.

CYP71A12 and CYP71A13 are required for the conversion of IAOx to IAN, which can be metabolized to camalexin or ICA. Our finding that EE-induced SAR is absent in *cyp71a12/a13*, although this mutant still accumulates wild-type levels of ICA after *B. cinerea* infection, suggests that this indolic metabolite is not the main contributor here. A way of obtaining definitive proof would be to test a mutant that lacks ICA exclusively and observe no defect in EE-induced SAR. However, given that ICA concentrations were also unaffected in *tmyb* and in *cyp71b6 aao1*, illustrating several redundant routes to ICA biosynthesis, such a mutant may be difficult to obtain. Interestingly, a role for indolic metabolites in Arabidopsis resistance against isolates of the necrotrophic fungus *P. cucumerina* has been reported (Sanchez-Vallet *et al.*, 2010). The *cyp79b2 cyp79b3* mutant was fully susceptible to *P. cucumerina* infection but camalexin and indole GSs played a minor role in resistance, implying the existence of other antifungal tryptophan derivatives. Strikingly, metabolite profiling after *P. cucumerina* infection revealed a significant accumulation of ICA, and mutants affected in biosynthesis of ICA conjugates were more susceptible to this pathogen (Sanchez-Vallet *et al.*, 2010; Gamir *et al.*, 2012; Pastorczyk *et al.*, 2020). There is thus evidence that ICA may contribute to defense against some fungal pathogens. The relatively weak yet significant toxicity of ICA towards *B. cinerea* BMM *in vitro* supports this hypothesis and requires further evaluation.

Egg extract-induced SAR also targets the oomycete *H. arabidopsidis* Noco2 in an NHP-dependent way and raises the question of the nature of plant defense compounds involved in this response. In Arabidopsis, basal immunity to *H. arabidopsidis* is activated by the detection of microbe-associated molecular patterns (Oome *et al.*, 2014) and involves the concerted action of Enhanced Disease Susceptibility1 (EDS1) and Phytoalexin Deficient4 (PAD4), followed by mobilization of the SA pathway (Rietz *et al.*, 2011). Interestingly, local pre-treatment with the molecular pattern nlp24 led to systemic resistance against *H. arabidopsidis* (Albert *et al.*, 2015). Although camalexin accumulates after *H. arabidopsidis* infection (Mert-Türk *et al.*, 2003), previous studies have shown that *pad3-1* and *cyp79b2 cyp79b3* do not show enhanced susceptibility, suggesting that camalexin and other tryptophan-derived metabolites are not crucial for resistance (Glazebrook *et al.*, 1997; Stuttmann *et al.*, 2011). Again, further work will be necessary to identify metabolites or defense proteins involved in EE-induced SAR against this oomycete.

Studies with *Pieris brassicae* have revealed that prior egg deposition primes plants for a better defense against hatching larvae and, interestingly, that this phenomenon depends on the SA pathway and requires ALD1 (Geiselhardt *et al.*, 2013; Pashalidou *et al.*, 2015; Bonnet *et al.*, 2017; Lortzing *et al.*, 2019; Valsamakias *et al.*, 2020). Our observation that *P. brassicae* larvae perform poorly on *B. cinerea*-infected plants may suggest that egg-induced SAR would be beneficial for the insect. However, in light of the

findings described in this article, the situation might be different in the context of natural oviposition on plants that become infested. Egg-induced priming of defenses might overcome the potential benefit of feeding on healthier plants. Further experiments will be needed to answer this question. Also, given that larval feeding creates open wounds that are potential entries for opportunistic pathogens, plants may have evolved egg-induced SAR to anticipate such threat.

That insect eggs protect *Arabidopsis* against *Pseudomonas syringae* (Hilfiker *et al.*, 2014), *B. cinerea* BMM and *H. arabidopsidis* Noco2 is remarkable given the different lifestyles of these pathogens. Intriguingly, treatment of *Arabidopsis* leaves with rhamnolipids was shown to induce resistance against the same three pathogens in an SA-dependent manner (Sanchez *et al.*, 2012). Rhamnolipids are produced by several bacterial species and are potent activators of immunity (Vatsa *et al.*, 2010). Similarly, we recently found that insect egg-derived PCs are responsible for the activation of immune responses, including SA accumulation, and that this response depends on LecRK-I.8 (Stahl *et al.*, 2020). We show here that EE-induced SAR against *B. cinerea* is also induced by PCs and requires LecRK-I.8. It would be interesting to test whether rhamnolipids and egg PCs inhibit pathogen growth through a similar mechanism. In addition, assays with different plant species, including crops, and leaf pathogens will be needed to explore the generality of egg- and PC-induced SAR. If validated, this may lead to the development of an efficient strategy to control a broad range of diseases.

In conclusion, this study shows that insect eggs activate a SAR targeting a necrotrophic fungus and an oomycete pathogen. This phenomenon extends to neighboring plants, requires the SA and NHP pathways, and may involve indolic metabolism. Whether insects, plants, or both benefit from such a SAR will require further studies, but this finding illustrates a fascinating aspect of plant–herbivore interactions.







Acknowledgements

This research was supported by a grant (310030_200372) from the Swiss National Science Foundation to PR, by the Less is More grant (847.13.006) of the Netherlands Organization for Scientific Research to GVdA and TMR, and by a grant (ZE467/6–2) of the German Research Foundation (DFG) to JZ. We thank Blaise Tissot and Caroline Gouhier-Darimont for maintenance of plants and insects, and Steve Lassueur for help with metabolite analyses. We thank N. Clay (Yale University, USA), E. Glawischignig (TUM München, Germany), I. Somssich (MPI Koeln, Germany) and Y. Zhang (University of British Columbia, CA) for sharing mutants. We thank the anonymous reviewers for useful comments on a previous version of the manuscript.

Author contributions

EA, ES, TMR, GVdA and PR conceived the research plans. EA, GG, ES, EB, JZ and TMR performed the experiments and analyzed the data. PR wrote the article with contributions from all the authors.

ORCID

Gaétan Glauser  <https://orcid.org/0000-0002-0983-8614>
Tom M. Raaymakers  <https://orcid.org/0000-0003-1056-7177>
Philippe Reymond  <https://orcid.org/0000-0002-3341-6200>
Elia Stahl  <https://orcid.org/0000-0002-2612-2669>
Guido Van den Ackerveken  <https://orcid.org/0000-0002-0183-8978>
Jürgen Zeier  <https://orcid.org/0000-0002-8703-5403>

Data availability

The data that support the findings of this study are available on request from the corresponding author.

References

- Albert I, Böhm H, Albert M, Feiler CE, Imkamp J, Wallmeroth N, Brancato C, Raaymakers TM, Oome S, Zhang H *et al.* 2015. An RLP23–SOBIR1–BAK1 complex mediates NLP-triggered immunity. *Nature Plants* 1: 15140.
- Balmer A, Pastor V, Glauser G, Mauch-Mani B. 2018. Tricarboxylates induce defense priming against bacteria in *Arabidopsis thaliana*. *Frontiers in Plant Science* 9: 1221.
- Bednarek P. 2012. Chemical warfare or modulators of defence responses – the function of secondary metabolites in plant immunity. *Current Opinion in Plant Biology* 15: 407–414.
- Bednarek P, Piślewska-Bednarek M, Loren V, van Themaat E, Maddula RK, Svatos A, Schulze-Lefert P. 2011. Conservation and clade-specific diversification of pathogen-inducible tryptophan and indole glucosinolate metabolism in *Arabidopsis thaliana* relatives. *New Phytologist* 192: 713–726.
- Bednarek P, Piślewska-Bednarek M, Svatos A, Schneider B, Doubsky J, Mansurova M, Humphry M, Consonni C, Panstruga R, Sanchez-Vallet A *et al.* 2009. A glucosinolate metabolism pathway in living plant cells mediates broad-spectrum antifungal defense. *Science* 323: 101–106.
- Beekwilder J, van Leeuwen W, van Dam NM, Bertossi M, Grandi V, Mizzi L, Soloviev M, Szabados L, Molthoff JW, Schipper B *et al.* 2008. The impact of the absence of aliphatic glucosinolates on insect herbivory in *Arabidopsis*. *PLoS ONE* 3: e2068.
- Birkenbihl RP, Diezel C, Somssich IE. 2012. *Arabidopsis* WRKY33 is a key transcriptional regulator of hormonal and metabolic responses toward *Botrytis cinerea* infection. *Plant Physiology* 159: 266–285.
- Bonnet C, Lassueur S, Ponzio C, Gols R, Dicke M, Reymond P. 2017. Combined biotic stresses trigger similar transcriptomic responses but contrasting resistance against a chewing herbivore in *Brassica nigra*. *BMC Plant Biology* 17: 127.
- Böttcher C, Chapman A, Fellermeier F, Choudhary M, Scheel D, Glawischignig E. 2014. The Biosynthetic pathway of indole-3-carbaldehyde and indole-3-carboxylic acid derivatives in *Arabidopsis*. *Plant Physiology* 165: 841–853.
- Bruessow F, Gouhier-Darimont C, Buchala A, Metraux J-P, Reymond P. 2010. Insect eggs suppress plant defence against chewing herbivores. *The Plant Journal* 62: 876–885.
- Buxdorf K, Yaffe H, Barda O, Levy M. 2013. The effects of glucosinolates and their breakdown products on necrotrophic fungi. *PLoS ONE* 8: e70771.
- Chen Y-C, Holmes EC, Rajniak J, Kim J-G, Tang S, Fischer CR, Mudgett MB, Sattely ES. 2018. N-hydroxy-pipecolic acid is a mobile metabolite that induces systemic disease resistance in *Arabidopsis*. *Proceedings of the National Academy of Sciences, USA* 115: E4920–E4929.
- Clay NK, Adio AM, Denoux C, Jander G, Ausubel FM. 2009. Glucosinolate metabolites required for an *Arabidopsis* innate immune response. *Science* 323: 95–101.
- Coates ME, Beynon JL. 2010. *Hyaloperonospora arabidopsidis* as a pathogen model. *Annual Review of Phytopathology* 48: 329–345.

- Conrath U. 2011. Molecular aspects of defence priming. *Trends in Plant Science* 16: 524–531.
- Dean R, van Kan JAL, Pretorius ZA, Hammond-Kosack KE, Di Pietro A, Spanu PD, Rudd JJ, Dickman M, Kahmann R, Ellis J *et al.* 2012. The top 10 fungal pathogens in molecular plant pathology. *Molecular Plant Pathology* 13: 414–430.
- Ding P, Rekhter D, Ding Y, Feussner K, Busta L, Haroth S, Xu S, Li X, Jetter R, Feussner I *et al.* 2016. Characterization of a pipecolic acid biosynthesis pathway required for systemic acquired resistance. *Plant Cell* 28: 2603–2615.
- Erb M, Reymond P. 2019. Molecular interactions between plants and insect herbivores. *Annual Review of Plant Biology* 70: 527–557.
- Fatouros NE, Pineda A, Huigens ME, Broekgaarden C, Shimwela MM, Figueroa Candia IA, Verbaarschot P, Bukovinsky T. 2014. Synergistic effects of direct and indirect defences on herbivore egg survival in a wild crucifer. *Proceedings of the Royal Society of London, Series B: Biological Sciences* 281: 20141254.
- Ferrari S, Galletti R, Denoux C, De Lorenzo G, Ausubel FM, Dewdney J. 2007. Resistance to *Botrytis cinerea* induced in Arabidopsis by elicitors is independent of salicylic acid, ethylene, or jasmonate signaling but requires PHYTOALEXIN DEFICIENT3. *Plant Physiology* 144: 367–379.
- Ferrari S, Plotnikova JM, De Lorenzo G, Ausubel FM. 2003. Arabidopsis local resistance to *Botrytis cinerea* involves salicylic acid and camalexin and requires EDS4 and PAD2, but not SID2, EDS5 or PAD4. *The Plant Journal* 35: 193–205.
- Forcat S, Bennett M, Grant M, Mansfield JW. 2010. Rapid linkage of indole carboxylic acid to the plant cell wall identified as a component of basal defence in Arabidopsis against *hrp* mutant bacteria. *Phytochemistry* 71: 870–876.
- Frerigmann H, Gigolashvili T. 2014. MYB34, MYB51, and MYB122 distinctly regulate indolic glucosinolate biosynthesis in *Arabidopsis thaliana*. *Molecular Plant* 7: 814–828.
- Frerigmann H, Glawischning E, Gigolashvili T. 2015. The role of MYB34, MYB51 and MYB122 in the regulation of camalexin biosynthesis in *Arabidopsis thaliana*. *Frontiers in Plant Science* 6: 654.
- Frerigmann H, Piślewska-Bednarek M, Sanchez-Vallet A, Molina A, Glawischning E, Gigolashvili T, Bednarek P. 2016. Regulation of pathogen-triggered tryptophan metabolism in *Arabidopsis thaliana* by MYB transcription factors and indole glucosinolate conversion products. *Molecular Plant* 9: 682–695.
- Gamir J, Pastor V, Cerezo M, Flors V. 2012. Identification of indole-3-carboxylic acid as mediator of priming against *Plectosphaerella cucumerina*. *Plant Physiology and Biochemistry* 61: 169–179.
- Garcion C, Lohmann A, Lamodière E, Catinot J, Buchala A, Doermann P, Metraux J-P. 2008. Characterization and biological function of the *ISOCHORISMATE SYNTHASE2* gene of Arabidopsis. *Plant Physiology* 147: 1279–1287.
- Geiselhardt S, Yoneya K, Blenn B, Drechsler N, Gershenzon J, Kunze R, Hilker M. 2013. Egg laying of Cabbage White butterfly (*Pieris brassicae*) on *Arabidopsis thaliana* affects subsequent performance of the larvae. *PLoS ONE* 8: e59661.
- Geuss D, Stelzer S, Lortzing T, Steppuhn A. 2017. *Solanum dulcamara*'s response to eggs of an insect herbivore comprises ovicidal hydrogen peroxide production. *Plant, Cell & Environment* 40: 2663–2677.
- Glauser G, Schweizer F, Turlings TCJ, Reymond P. 2012. Rapid profiling of intact glucosinolates in Arabidopsis leaves by UHPLC-QTOFMS using a charged surface hybrid column. *Phytochemical Analysis* 23: 520–528.
- Glazebrook J, Zook M, Mert F, Kagan I, Rogers EE, Crute IR, Holub EB, Hammerschmidt R, Ausubel FM. 1997. Phytoalexin-deficient mutants of Arabidopsis reveal that PAD4 encodes a regulatory factor and that four PAD genes contribute to downy mildew resistance. *Genetics* 146: 381–392.
- Gouhier-Darimont C, Schmiesing A, Bonnet C, Lassueur S, Reymond P. 2013. Signalling of *Arabidopsis thaliana* response to *Pieris brassicae* eggs shares similarities with PAMP-triggered immunity. *Journal of Experimental Botany* 64: 665–674.
- Gouhier-Darimont C, Stahl E, Glauser G, Reymond P. 2019. The Arabidopsis lectin receptor kinase LecRK-I.8 is involved in insect egg perception. *Frontiers Plant Science* 10: 623.
- Griese E, Caarls L, Bassetti N, Mohammadin S, Verbaarschot P, Bukovinsky K, Kiss G, Poelman EH, Gols R, Schranz ME, Fatouros NE. 2021. Insect egg-killing: a new front on the evolutionary arms-race between brassicaceous plants and pierid butterflies. *New Phytologist* 230: 341–353.
- Griese E, Dicke M, Hilker M, Fatouros NE. 2017. Plant response to butterfly eggs: inducibility, severity and success of egg-killing leaf necrosis depends on plant genotype and egg clustering. *Scientific Reports* 7: 7316.
- Hartmann M, Kim D, Bernsdorff F, Ajami-Rashidi Z, Scholten N, Schreiber S, Zeier T, Schuck S, Reichel-Deland V, Zeier J. 2017. Biochemical principles and functional aspects of pipecolic acid biosynthesis in plant immunity. *Plant Physiology* 174: 124–153.
- Hartmann M, Zeier J. 2019. N-hydroxypipecolic acid and salicylic acid: a metabolic duo for systemic acquired resistance. *Current Opinion in Plant Biology* 50: 44–57.
- Hartmann M, Zeier T, Bernsdorff F, Reichel-Deland V, Kim D, Hohmann M, Scholten N, Schuck S, Bräutigam A, Hölzel T *et al.* 2018. Flavin monooxygenase-generated N-hydroxypipecolic acid is a critical element of plant systemic immunity. *Cell* 173: 456–469.
- He Y, Xu J, Wang X, He X, Wang Y, Zhou J, Zhang S, Meng X. 2019. The Arabidopsis pleiotropic drug resistance transporters PEN3 and PDR12 mediate camalexin secretion for resistance to *Botrytis cinerea*. *Plant Cell* 31: 2206–2222.
- Hilfiker O, Groux R, Bruessow F, Kiefer K, Zeier J, Reymond P. 2014. Insect eggs induce a systemic acquired resistance in Arabidopsis. *The Plant Journal* 80: 1085–1094.
- Hilker M, Fatouros NE. 2015. Plant responses to insect egg deposition. *Annual Review of Entomology* 60: 493–515.
- Hilker M, Kobs C, Varama M, Schrank K. 2002. Insect egg deposition induces *Pinus sylvestris* to attract egg parasitoids. *Journal of Experimental Biology* 205: 455–461.
- Howe GA, Jander G. 2008. Plant immunity to insect herbivores. *Annual Review of Plant Biology* 59: 41–66.
- Huang WE, Huang L, Preston GM, Naylor M, Carr JP, Li Y, Singer AC, Whiteley AS, Wang H. 2006. Quantitative in situ assay of salicylic acid in tobacco leaves using a genetically modified biosensor strain of *Acinetobacter* sp. ADP1. *The Plant Journal* 46: 1073–1083.
- Huang WE, Wang H, Zheng H, Huang L, Singer AC, Thompson I, Whiteley AS. 2005. Chromosomally located gene fusions constructed in *Acinetobacter* sp. ADP1 for the detection of salicylate. *Environmental Microbiology* 7: 1339–1348.
- Jung HW, Tschaplinski TJ, Wang L, Glazebrook J, Greenberg JT. 2009. Priming in systemic plant immunity. *Science* 324: 89–91.
- Katz E, Nisani S, Yadav BS, Woldemariam MG, Shai B, Obolski U, Ehrlich M, Shani E, Jander G, Chamovitz DA. 2015. The glucosinolate breakdown product indole-3-carbinol acts as an auxin antagonist in roots of *Arabidopsis thaliana*. *The Plant Journal* 82: 547–555.
- Kavitha A, Prabhakar P, Vijayalakshmi M, Venkateswarlu Y. 2010. Purification and biological evaluation of the metabolites produced by *Streptomyces* sp. TK-VL_333. *Research in Microbiology* 161: 335–345.
- Kettles GJ, Drurey C, Schoonbeek H-J, Maule AJ, Hogenhout SA. 2013. Resistance of *Arabidopsis thaliana* to the green peach aphid, *Myzus persicae*, involves camalexin and is regulated by microRNAs. *New Phytologist* 198: 1178–1190.
- Khare D, Choi H, Huh SU, Bassin B, Kim J, Martinoia E, Sohn KH, Paek K-H, Lee Y. 2017. Arabidopsis ABCG34 contributes to defense against necrotrophic pathogens by mediating the secretion of camalexin. *Proceedings of the National Academy of Sciences, USA* 114: E5712–E5720.
- Kim JH, Lee BW, Schroeder FC, Jander G. 2008. Identification of indole glucosinolate breakdown products with antifeedant effects on *Myzus persicae* (green peach aphid). *The Plant Journal* 54: 1015–1026.
- Kliebenstein DJ, Rowe HC, Denby KJ. 2005. Secondary metabolites influence Arabidopsis/*Botrytis* interactions: variation in host production and pathogen sensitivity. *The Plant Journal* 44: 25–36.
- Little D, Gouhier-Darimont C, Bruessow F, Reymond P. 2007. Oviposition by pierid butterflies triggers defense responses in Arabidopsis. *Plant Physiology* 143: 784–800.
- Liu S, Kracher B, Ziegler J, Birkenbihl RP, Somssich IE. 2015. Negative regulation of ABA signaling by WRKY33 is critical for Arabidopsis immunity towards *Botrytis cinerea* 2100. *eLife* 4: e07295.
- Liu Y, Sun T, Sun Y, Zhang Y, Radojčić A, Ding Y, Tian H, Huang X, Lan J, Chen S *et al.* 2020. Diverse roles of the salicylic acid receptors NPR1 and NPR3/NPR4 in plant immunity. *Plant Cell* 32: 4002–4016.

- Lortzing T, Kunze SA, Hilker M, Lortzing V. 2020. Arabidopsis, tobacco, nightshade and elm take insect eggs as herbivore alarm and show similar transcriptomic alarm responses. *Scientific Reports* 10: 16281.
- Lortzing V, Oberländer J, Lortzing T, Tohge T, Steppuhn A, Kunze R, Hilker M. 2019. Insect egg deposition renders plant defence against hatching larvae more effective in a salicylic acid-dependent manner. *Plant, Cell & Environment* 42: 1019–1032.
- Maier BA, Kiefer P, Field CM, Hemmerle L, Bortfeld-Miller M, Emmenegger B, Schäfer M, Pfeilmeier S, Sunagawa S, Vogel CM *et al.* 2021. A general non-self response as part of plant immunity. *Nature Plants* 7: 696–705.
- Mert-Türk F, Bennett MH, Mansfield JW, Holub E. 2003. Camalexin accumulation in *Arabidopsis thaliana* following abiotic elicitation or inoculation with virulent or avirulent *Hyaloperonospora parasitica*. *Physiological and Molecular Plant Pathology* 62: 137–145.
- Mucha S, Heinzlmeir S, Kriechbaumer V, Strickland B, Kirchhelle C, Choudhary M, Kowalski N, Eichmann R, Hueckelhoven R, Grill E *et al.* 2019. The formation of a camalexin biosynthetic metabolon. *Plant Cell* 31: 2697–2710.
- Návarová H, Bernsdorff F, Döring A-C, Zeier J. 2012. Pipecolic acid, an endogenous mediator of defense amplification and priming, is a critical regulator of inducible plant immunity. *Plant Cell* 24: 5123–5141.
- Nawrath C, Métraux JP. 1999. Salicylic acid induction-deficient mutants of *Arabidopsis* express *PR-2* and *PR-5* and accumulate high levels of camalexin after pathogen inoculation. *Plant Cell* 11: 1393–1404.
- Nie P, Li X, Wang S, Guo J, Zhao H, Niu D. 2017. Induced systemic resistance against *Botrytis cinerea* by *Bacillus cereus* AR156 through a JA/ET- and NPR1-dependent signaling pathway and activates PAMP-triggered immunity in *Arabidopsis*. *Frontiers in Plant Science* 8: 238.
- Oome S, Raaymakers TM, Cabral A, Samwel S, Böhm H, Albert I, Nürnberger T, Van den Ackerveken G. 2014. Nep1-like proteins from three kingdoms of life act as a microbe-associated molecular pattern in *Arabidopsis*. *Proceedings of the National Academy of Sciences, USA* 111: 16955–16960.
- Orlovskis Z, Reymond P. 2020. *Pieris brassicae* eggs trigger interplant systemic acquired resistance against a foliar pathogen in *Arabidopsis*. *New Phytologist* 228: 1652–1661.
- Pashalidou FG, Fatouros NE, van Loon JJA, Dicke M, Gols R. 2015. Plant-mediated effects of butterfly egg deposition on subsequent caterpillar and pupal development, across different species of wild Brassicaceae. *Ecological Entomology* 40: 444–450.
- Pastorzcyk M, Kosaka A, Piślewska-Bednarek M, López G, Frerigmann H, Kułak K, Glawischnig E, Molina A, Takano Y, Bednarek P. 2020. The role of CYP71A12 monooxygenase in pathogen-triggered tryptophan metabolism and *Arabidopsis* immunity. *New Phytologist* 225: 400–412.
- Pedras MSC, Hossain S. 2011. Interaction of cruciferous phytoanticipins with plant fungal pathogens: indole glucosinolates are not metabolized but the corresponding desulfo-derivatives and nitriles are. *Phytochemistry* 72: 2308–2316.
- Pedras MSC, Hossain S, Snitynsky RB. 2011. Detoxification of cruciferous phytoalexins in *Botrytis cinerea*: spontaneous dimerization of a camalexin metabolite. *Phytochemistry* 72: 199–206.
- Pieterse CMJ, Van der Does D, Zamioudis C, Leon-Reyes A, Van Wees SCM. 2012. Hormonal modulation of plant immunity. *Annual Review of Cell and Developmental Biology* 28: 489–521.
- Rajniak J, Barco B, Clay NK, Sattely ES. 2015. A new cyanogenic metabolite in *Arabidopsis* required for inducible pathogen defence. *Nature* 525: 376–379.
- Reymond P. 2013. Perception, signaling and molecular basis of oviposition-mediated plant responses. *Planta* 238: 247–258.
- Reymond P, Weber H, Damond M, Farmer EE. 2000. Differential gene expression in response to mechanical wounding and insect feeding in *Arabidopsis*. *Plant Cell* 12: 707–720.
- Rietz S, Stamm A, Malonek S, Wagner S, Becker D, Medina-Escobar N, Vlot AC, Feys BJ, Niefind K, Parker JE. 2011. Different roles of Enhanced Disease Susceptibility1 (EDS1) bound to and dissociated from Phytoalexin Deficient4 (PAD4) in *Arabidopsis* immunity. *New Phytologist* 191: 107–119.
- Sanchez L, Courteaux B, Hubert J, Kauffmann S, Renault J-H, Clément C, Baillieul F, Dorey S. 2012. Rhamnolipids elicit defense responses and induce disease resistance against biotrophic, hemibiotrophic, and necrotrophic pathogens that require different signaling pathways in *Arabidopsis* and highlight a central role for salicylic acid. *Plant Physiology* 160: 1630–1641.
- Sanchez-Vallet A, Ramos B, Bednarek P, López G, Piślewska-Bednarek M, Schulze-Lefert P, Molina A. 2010. Tryptophan-derived secondary metabolites in *Arabidopsis thaliana* confer non-host resistance to necrotrophic *Plectosphaerella cucumerina* fungi. *The Plant Journal* 63: 115–127.
- Schuhegger R, Nafisi M, Mansourova M, Petersen BL, Olsen CE, Svatos A, Halkier BA, Glawischnig E. 2006. CYP71B15 (PAD3) catalyzes the final step in camalexin biosynthesis. *Plant Physiology* 141: 1248–1254.
- Shah J, Zeier J. 2013. Long-distance communication and signal amplification in systemic acquired resistance. *Frontiers in Plant Science* 4: 30.
- Stahl E, Bellwon P, Huber S, Schlaeppli K, Bernsdorff F, Vallat-Michel A, Mauch F, Zeier J. 2016. Regulatory and functional aspects of indolic metabolism in plant systemic acquired resistance. *Molecular Plant* 9: 662–681.
- Stahl E, Brillatz T, Ferreira Queiroz E, Marcourt L, Schmieging A, Hilfiker O, Riezman I, Riezman H, Wolfender J-L, Reymond P. 2020. Phosphatidylcholines from *Pieris brassicae* eggs activate an immune response in *Arabidopsis*. *eLife* 9: e60293.
- Stefanato F, Abou-Mansour E, Buchala A, Kretschmer M, Mosbach A, Hahn M, Bochet CG, Métraux J-P, Schoonbeek H. 2009. The ABC transporter BcatrB from *Botrytis cinerea* exports camalexin and is a virulence factor on *Arabidopsis thaliana*. *The Plant Journal* 58: 499–510.
- Sticher L, Mauch-Mani B, Métraux JP. 1997. Systemic acquired resistance. *Annual Review of Phytopathology* 35: 235–270.
- Stuttman J, Hubberten H-M, Rietz S, Kaur J, Muskett P, Guerois R, Bednarek P, Hoefgen R, Parker JE. 2011. Perturbation of *Arabidopsis* amino acid metabolism causes incompatibility with the adapted biotrophic pathogen *Hyaloperonospora arabidopsidis*. *Plant Cell* 23: 2788–2803.
- Tsuji J, Jackson EP, Gage DA, Hammerschmidt R, Somerville SC. 1992. Phytoalexin accumulation in *Arabidopsis thaliana* during the hypersensitive reaction to *Pseudomonas syringae* pv *syringae*. *Plant Physiology* 98: 1304–1309.
- Valsamakis G, Bittner N, Fatouros NE, Kunze R, Hilker M, Lortzing V. 2020. Priming by timing: *arabidopsis thaliana* adjusts its priming response to *Lepidoptera* eggs to the time of larval hatching. *Frontiers in Plant Science* 11: 619589.
- van Kan JAL, Shaw MW, Grant-Downton RT. 2014. *Botrytis* species: relentless necrotrophic thugs or endophytes gone rogue? *Molecular Plant Pathology* 15: 957–961.
- Vatsa P, Sanchez L, Clément C, Baillieul F, Dorey S. 2010. Rhamnolipid biosurfactants as new players in animal and plant defense against microbes. *International Journal of Molecular Sciences* 11: 5095–5108.
- Veloso J, van Kan JAL. 2018. Many shades of grey in *Botrytis*-host plant interactions. *Trends in Plant Science* 23: 613–622.
- Vlot AC, Dempsey DA, Klessig DF. 2009. Salicylic acid, a multifaceted hormone to combat disease. *Annual Review of Phytopathology* 47: 177–206.
- Wu J, Baldwin IT. 2010. New insights into plant responses to the attack from insect herbivores. *Annual Review of Genetics* 44: 1–24.
- Xu J, Meng J, Meng X, Zhao Y, Liu J, Sun T, Liu Y, Wang Q, Zhang S. 2016. Pathogen-responsive MPK3 and MPK6 reprogram the biosynthesis of indole glucosinolates and their derivatives in *Arabidopsis* immunity. *Plant Cell* 28: 1144–1162.
- Zeier J. 2021. Metabolic regulation of systemic acquired resistance. *Current Opinion in Plant Biology* 62: 102050.
- Zhang W, Corwin JA, Copeland D, Feusier J, Eshbaugh R, Chen F, Atwell S, Kliebenstein DJ. 2017. Plastic transcriptomes stabilize immunity to pathogen diversity: the jasmonic acid and salicylic acid networks within the *Arabidopsis*/*Botrytis* pathosystem. *Plant Cell* 29: 2727–2752.
- Zhao Y, Hull AK, Gupta NR, Goss KA, Alonso JM, Ecker JR, Normanly J, Chory J, Celenza JL. 2002. Trp-dependent auxin biosynthesis in *Arabidopsis*: involvement of cytochrome P450s CYP79B2 and CYP79B3. *Genes & Development* 16: 3100–3112.
- Zhou J, Wang X, He Y, Sang T, Wang P, Dai S, Zhang S, Meng X. 2020. Differential phosphorylation of the transcription factor WRKY33 by the protein kinases CPK5/CPK6 and MPK3/MPK6 cooperatively regulates camalexin biosynthesis in *Arabidopsis*. *Plant Cell* 32: 2621–2638.
- Zhou J-M, Zhang Y. 2020. Plant immunity: danger perception and signaling. *Cell* 181: 978–989.

Zimmerli L, Métraux JP, Mauch-Mani B. 2001. β -Aminobutyric acid-induced protection of *Arabidopsis* against the necrotrophic fungus *Botrytis cinerea*. *Plant Physiology* 126: 517–523.

Supporting Information

Additional Supporting Information may be found online in the Supporting Information section at the end of the article.

Fig. S1 Egg extract (EE) treatment reduces *Botrytis cinerea* growth in distal leaves.

Fig. S2 Time course of EE-induced reduction of *B. cinerea* infection.

Fig. S3 Salicylic acid (SA) quantification in SA biosynthesis mutants.

Fig. S4 Exogenous SA infiltration does not trigger EE-induced systemic acquired resistance (SAR).

Fig. S5 Glucosinolates concentrations in EE- and *B. cinerea*-treated plants.

Fig. S6 Indole-3-carboxylic acid (ICA) accumulates in response to *B. cinerea* infection.

Fig. S7 ICA conjugates accumulate in response to EE treatment.

Fig. S8 EE induces camalexin accumulation in local leaves.

Fig. S9 Early time course of camalexin accumulation.

Fig. S10 Camalexin concentrations in various indolic mutants.

Methods S1 Lines used in this study.

Methods S2 Measurement of *B. cinerea* growth by quantitative polymerase chain reaction (qPCR).

Methods S3 Metabolite analyses.

Table S1 Replicate numbers and summary statistics.

Table S2 Time-course of single glucosinolate species accumulation.

Table S3 Single glucosinolate species in Col-0 and the *myb* mutant.

Please note: Wiley Blackwell are not responsible for the content or functionality of any Supporting Information supplied by the authors. Any queries (other than missing material) should be directed to the *New Phytologist* Central Office.



About New Phytologist

- *New Phytologist* is an electronic (online-only) journal owned by the New Phytologist Foundation, a **not-for-profit organization** dedicated to the promotion of plant science, facilitating projects from symposia to free access for our Tansley reviews and Tansley insights.
- Regular papers, Letters, Viewpoints, Research reviews, Rapid reports and both Modelling/Theory and Methods papers are encouraged. We are committed to rapid processing, from online submission through to publication 'as ready' via *Early View* – our average time to decision is <26 days. There are **no page or colour charges** and a PDF version will be provided for each article.
- The journal is available online at Wiley Online Library. Visit **www.newphytologist.com** to search the articles and register for table of contents email alerts.
- If you have any questions, do get in touch with Central Office (np-centraloffice@lancaster.ac.uk) or, if it is more convenient, our USA Office (np-usaoffice@lancaster.ac.uk)
- For submission instructions, subscription and all the latest information visit **www.newphytologist.com**

***New Phytologist* Supporting Information**

Article title: Insect eggs trigger systemic acquired resistance against a fungal and an oomycete pathogen

Authors: Esteban Alfonso, Elia Stahl, Gaétan Glauser, Etienne Bellani, Tom M. Raaymakers, Guido Van den Ackerveken, Jürgen Zeier and Philippe Reymond

Article acceptance date: 05 September 2021

The following Supporting Information is available for this article:

Fig. S1 EE treatment reduces *Botrytis cinerea* growth in distal leaves.

Fig. S2 Time course of EE-induced reduction of *Botrytis cinerea* infection.

Fig. S3 SA quantification in SA biosynthesis mutants.

Fig. S4 Exogenous SA infiltration does not trigger EE-induced SAR.

Fig. S5 Glucosinolates levels in EE- and *Botrytis cinerea*-treated plants.

Fig. S6 ICA accumulates in response to *Botrytis cinerea* infection.

Fig. S7 ICA conjugates accumulate in response to EE treatment.

Fig. S8 EE induces camalexin accumulation in local leaves.

Fig. S9 Early time course of camalexin accumulation.

Fig. S10 Camalexin levels in various indolic mutants.

Table S1 Replicate numbers and summary statistics (see separate file).

Table S2 Time-course of single glucosinolate species accumulation.

Table S3 Single glucosinolate species in Col-0 and *tmyb* mutant.

Methods S1 Lines used in this study.

Methods S2 Measurement of *Botrytis cinerea* growth by QPCR.

Methods S3 Metabolite analyses.

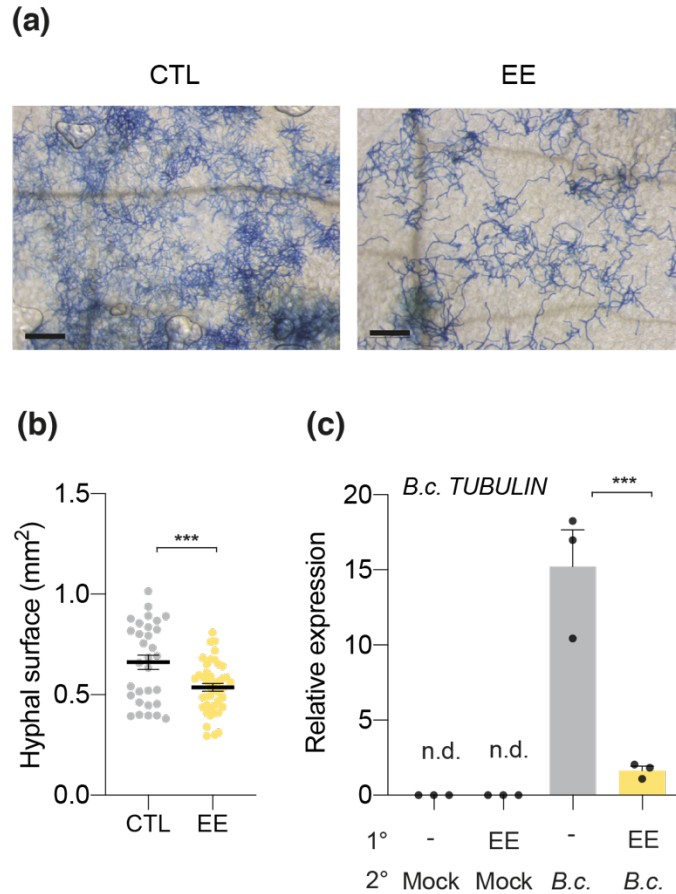


Fig. S1 Egg extract treatment reduces *Botrytis cinerea* growth in distal leaves. (a) Photographs of stained hyphae on control plants (top) and plants pretreated with *Pieris brassicae* egg extract (EE) (bottom, distal leaf), 2 days post-inoculation. Scale bar: 200 μ m. (b) Plants were pretreated with EE and hyphal growth was measured 2 days after inoculation. Hyphae were stained by trypan blue and the surface of hyphae was quantified with ImageJ. Means \pm SE of three independent experiments are shown (n = 8-14 per experiment). Significant differences between control and treated plants are indicated (linear mixed model, *** $P < 0.001$). (c) Expression of the *B. cinerea* tubulin gene in distal leaves. Local leaves (1°) were either treated with EE for 5 days or not treated (-). Distal leaves (2°) were then inoculated with PDB (Mock) or *B. cinerea* spore suspension (*B.c.*) for 2 days. Means \pm SE of three independent experiments are shown (n = 10-12 per experiment). Significant differences between control and treated plants are indicated (linear mixed model, *** $P < 0.001$. n.d. not determined).

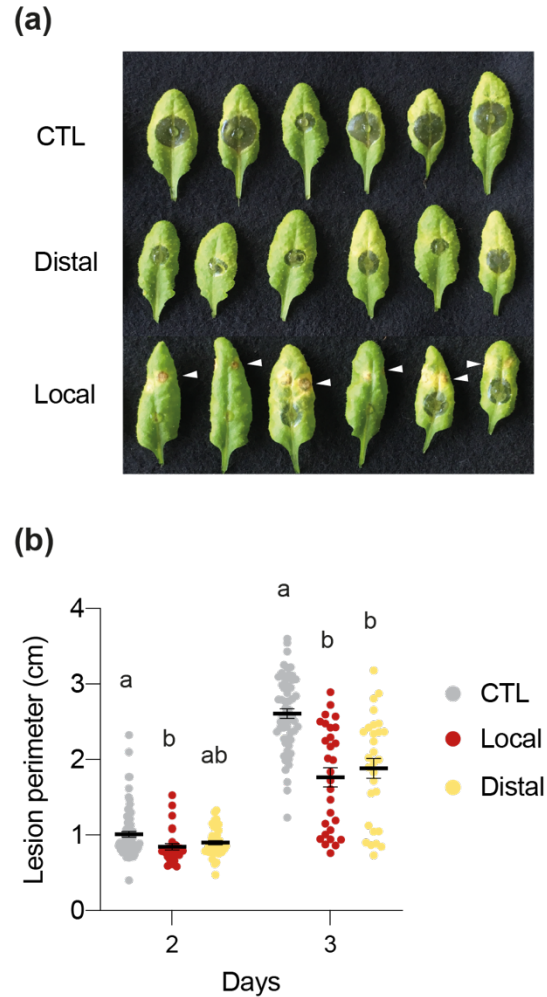


Fig. S2 Time course of egg extract-induced reduction of *Botrytis cinerea* infection. (a) A solution of *B. cinerea* spores was deposited on untreated plants (CTL), on leaves distal to *Pieris brassicae* egg extract (EE)-treated leaves, or on EE-treated leaves. White arrows indicate the application site of the EE. Photographs were taken 3 days after infection. (b) Lesion perimeter measurement of control leaves, EE-treated leaves and leaves distal from EE-treated plants. Means \pm SE of three independent experiments are shown (n = 8-37 per experiment). For each time point, different letters indicate significant differences at $P < 0.05$ (ANOVA followed by Tukey's Honest Significant Difference test). Dots indicate individual values.

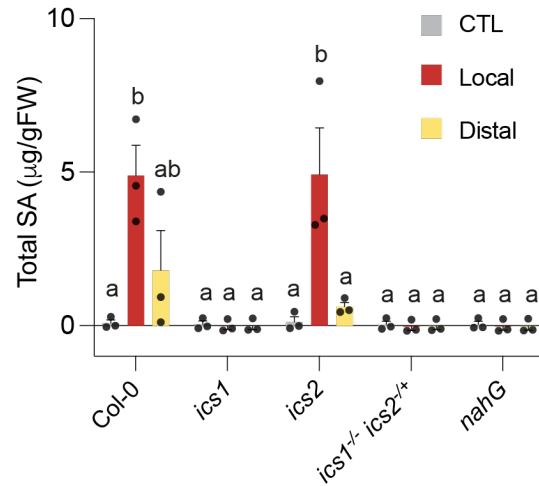


Fig. S3 Salicylic acid (SA) quantification in SA biosynthesis mutants. Total SA was measured in untreated plants (CTL), *Pieris brassicae* egg extract (EE)-treated leaves (Local) and in leaves distal to EE-treated leaves (Distal) after 5 days. Means \pm SE of three independent experiments are shown (n = 6 per experiment). Different letters indicate significant difference between treatments within genotypes at $P < 0.05$ (ANOVA followed by Tukey's Honest Significant Difference test).

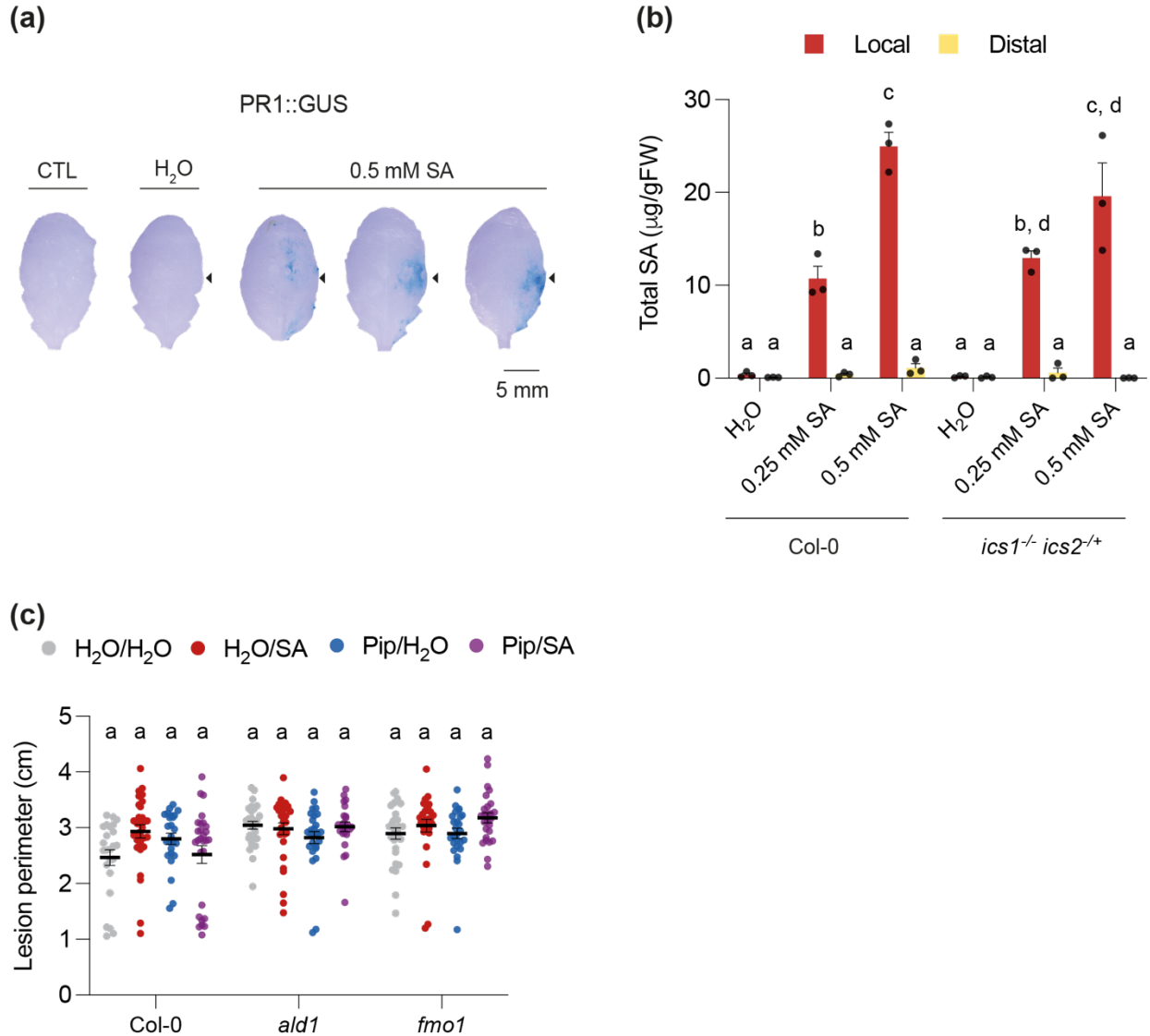


Fig. S4 Exogenous salicylic acid (SA) infiltration does not trigger egg extract-induced systemic acquired resistance. (a). Infiltration of H₂O and 0.5 mM SA in PR1::GUS reporter line. Black triangles indicate which half of the leaf was infiltrated. For SA infiltration, three representative images from different plants are shown. CTL, untreated. (b). Plant genotypes were infiltrated with H₂O, 0.25 mM and 0.5 mM of SA in the abaxial surface of two leaves per plant for 4 h before SA quantification in local (infiltrated leaves) and distal leaves. Means ± SE of three independent experiments are shown (n = 6 per experiment). The double mutant *ics1 ics2* was homozygous for *ics1* (^{-/-}) and heterozygous for *ics2* (^{+/-}). For each genotype and location, different letters indicate significant differences between treatments in local leaves at *P*<0.05 (ANOVA followed by Tukey's Honest Significant Difference test) (c). H₂O or 1 mM Pip solution was applied to the soil 24 h prior infection with *Botrytis cinerea* for 3 days. H₂O or 0.25 mM SA were infiltrated in two leaves per plant 4 h prior infection. Means ± SE of three independent experiments are shown (n = 6-12 per experiment). For each genotype, different letters indicate significant differences at *P*<0.05 (ANOVA followed by Tukey's Honest Significant Difference test). Dots indicate individual values.

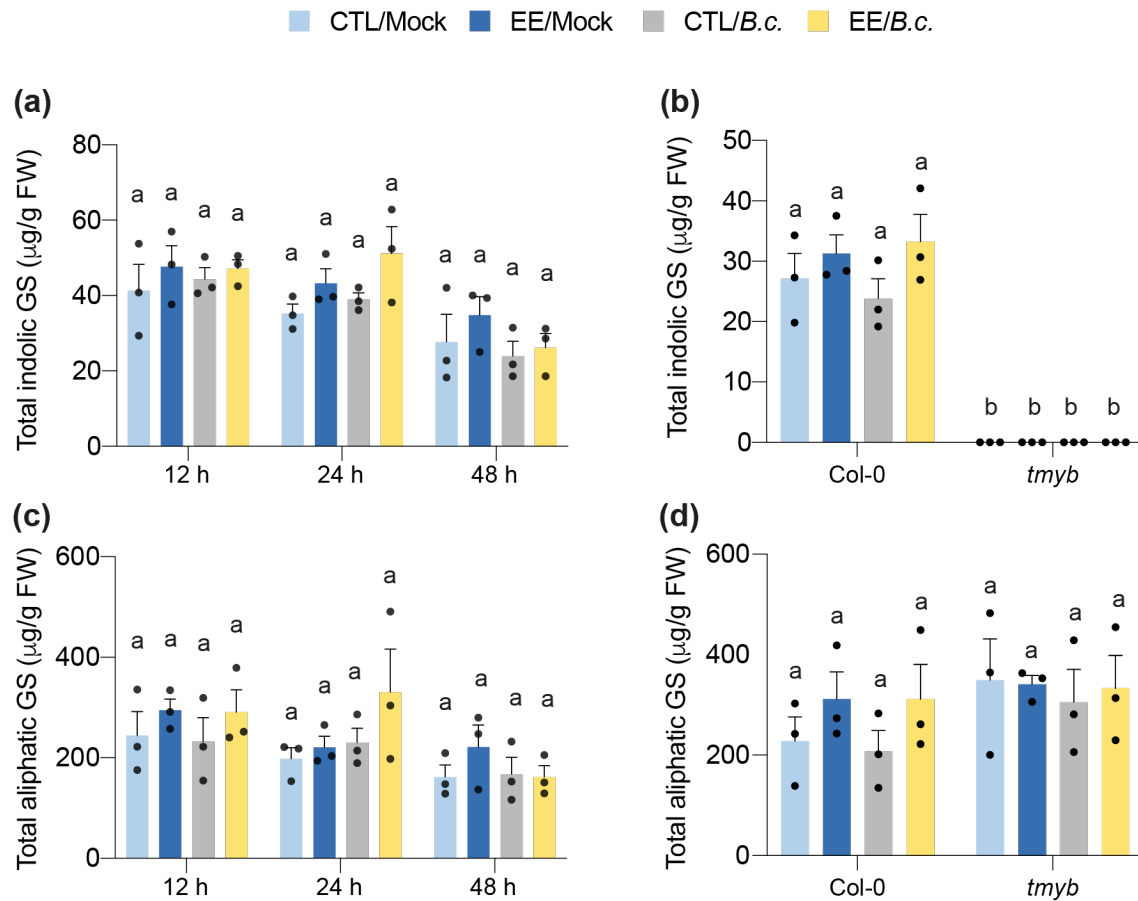


Fig. S5 Glucosinolates levels in egg extract- and *Botrytis cinerea*-treated plants. Levels of indolic glucosinolates (a,b) and aliphatic glucosinolates (c,d) were quantified in distal leaves from 12 h to 48 h after *B. cinerea* infection in Col-0 (a,c) or after 24 h in Col-0 and *tmyb* (b,d). Local leaves were pretreated with *Pieris brassicae* egg extract (EE) for 5 days or left untreated (CTL) and then distal leaves were infected with *B. cinerea* (*B.c.*) or a mock solution (Mock). Means \pm SE of three independent experiments are shown (n = 10-12 per experiment). For each time point (a,c) or between genotypes (b,d), different letters indicate significant differences at $P < 0.05$ (ANOVA followed by Tukey's Honest Significant Difference test). *tmyb* = *myb34 myb51 myb122*.

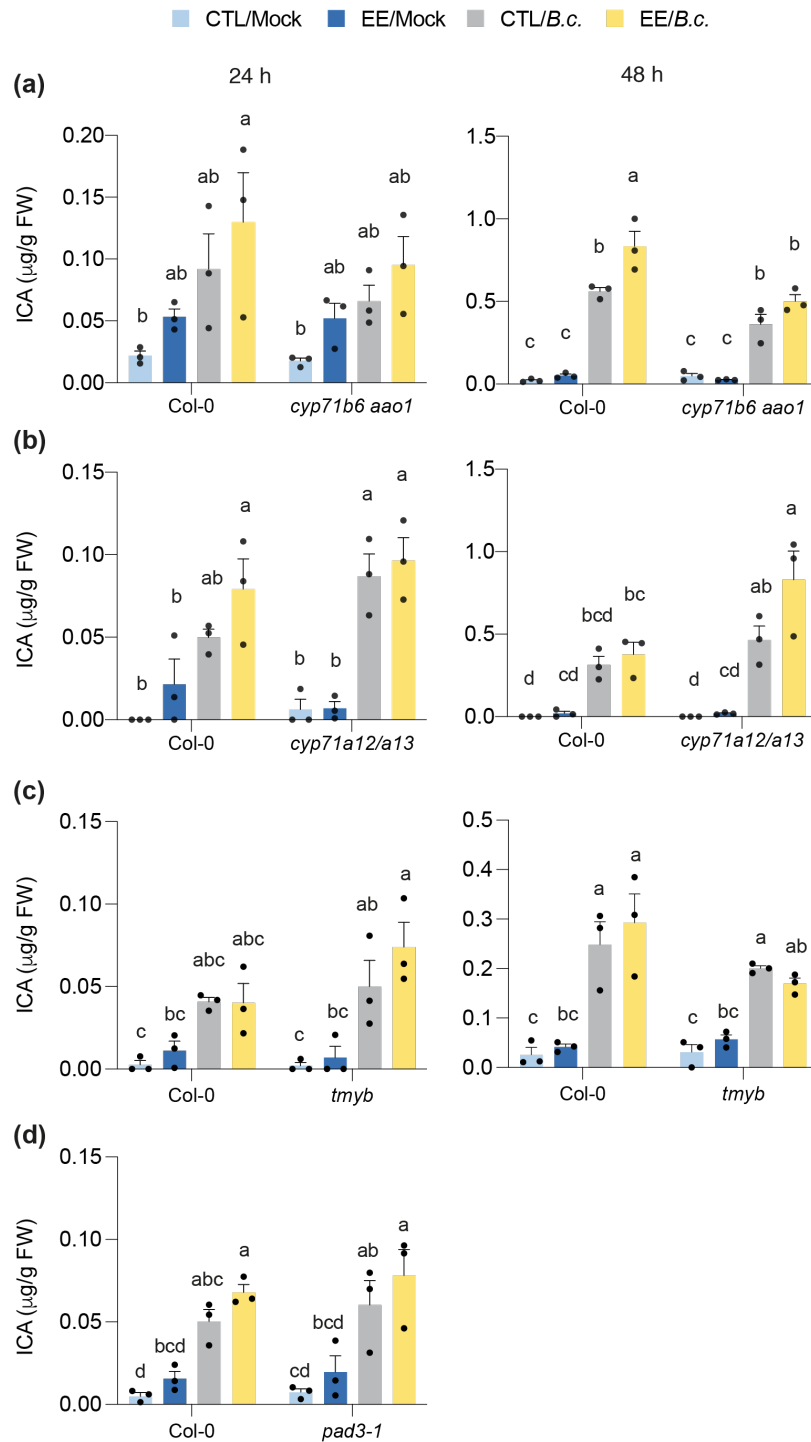


Fig. S6 Indole carboxylic acid (ICA) accumulates in response to *Botrytis cinerea* infection. (a-d) Levels of ICA were quantified in distal leaves from 24 h and 48 h after *B. cinerea* infection. Local leaves were pretreated with *Pieris brassicae* egg extract (EE) for 5 days or left untreated (CTL) and then distal leaves were infected with *B. cinerea* (*B.c.*) or a mock solution (Mock). Means \pm SE of three independent experiments are shown (n = 10-12 per experiment). Different letters indicate significant differences at $P < 0.05$ (ANOVA followed by Tukey's Honest Significant Difference test). *tmyb* = *myb34 myb51 myb122*.

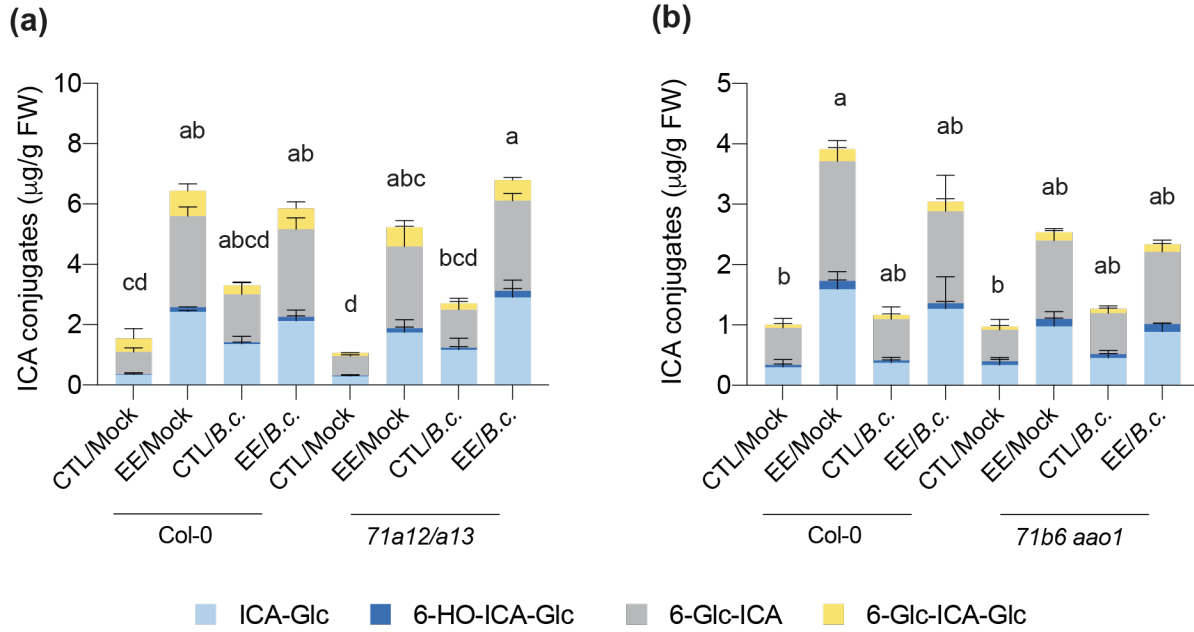


Fig. S7 Indole carboxylic acid (ICA) conjugates accumulate in response to egg extract treatment. (a,b) Levels of ICA conjugates were quantified in distal leaves 48 h after *Botrytis cinerea* infection. Local leaves were pretreated with *Pieris brassicae* egg extract (EE) for 5 days or left untreated (CTL) and then distal leaves were infected with *B. cinerea* (*B.c.*) or a mock solution (Mock). Means \pm SE of three independent experiments are shown (n = 10-12 per experiment). Different letters indicate significant differences at $P < 0.05$ (ANOVA followed by Tukey's Honest Significant Difference test).

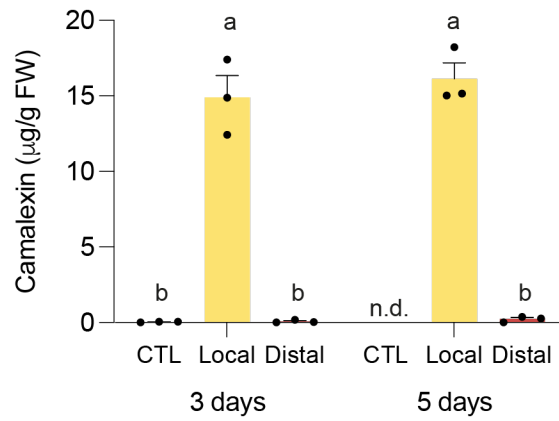


Fig. S8 Egg extract induces camalexin accumulation in local leaves. Levels of camalexin were quantified in local and distal leaves 3 and 5 days after *Pieris brassicae* egg extract treatment. Control (CTL) leaves were untreated. Means \pm SE of three independent experiments are shown (n = 10-12 per experiment). Different letters indicate significant differences at $P < 0.05$ (ANOVA followed by Tukey's Honest Significant Difference test). n.d., not determined.

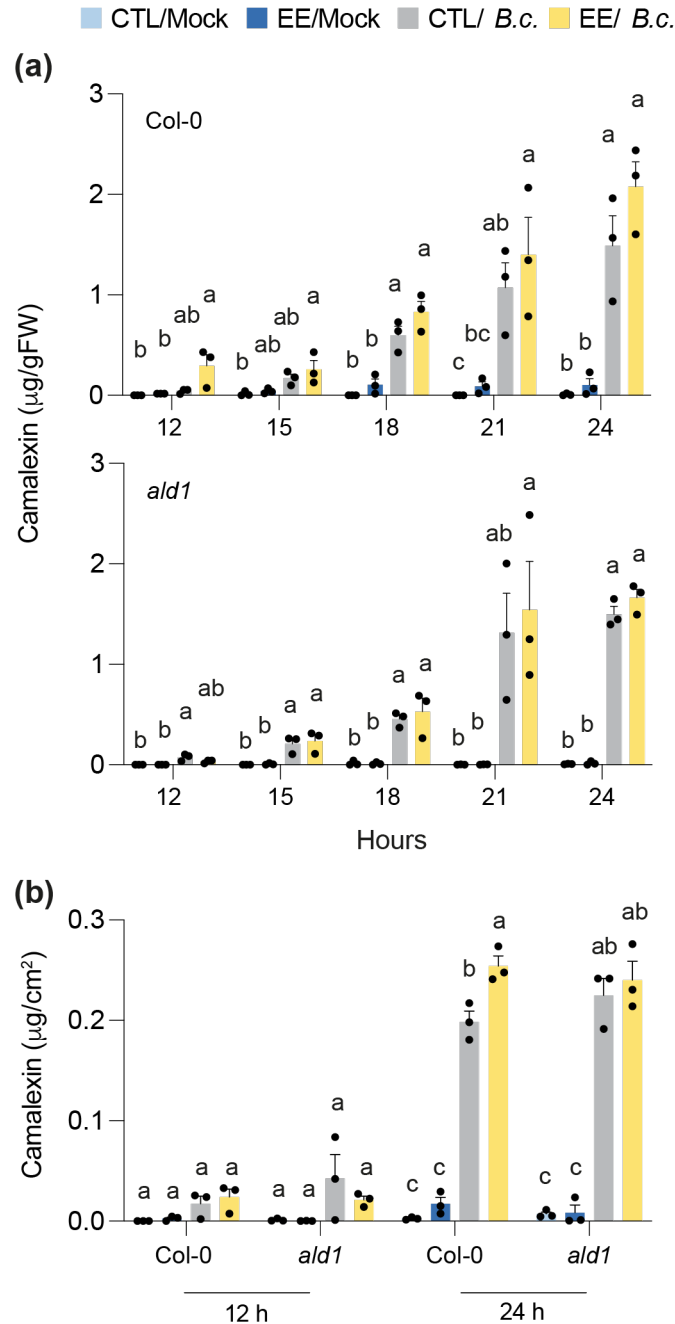


Fig. S9 Early time course of camalexin accumulation. Levels of camalexin were quantified in distal leaves from 12 h to 24 h after *Botrytis cinerea* infection. Local leaves were pretreated with *Pieris brassicae* egg extract (EE) for 5 days or left untreated (CTL) and then distal leaves were infected with *B. cinerea* (*B.c.*) or a mock solution (Mock). (a) Total and (b) leaf surface camalexin was analyzed. Means \pm SE of three independent experiments are shown (n = 8-12 per experiment). For each time point, different letters indicate significant differences at $P < 0.05$ (ANOVA followed by Tukey's Honest Significant Difference test).

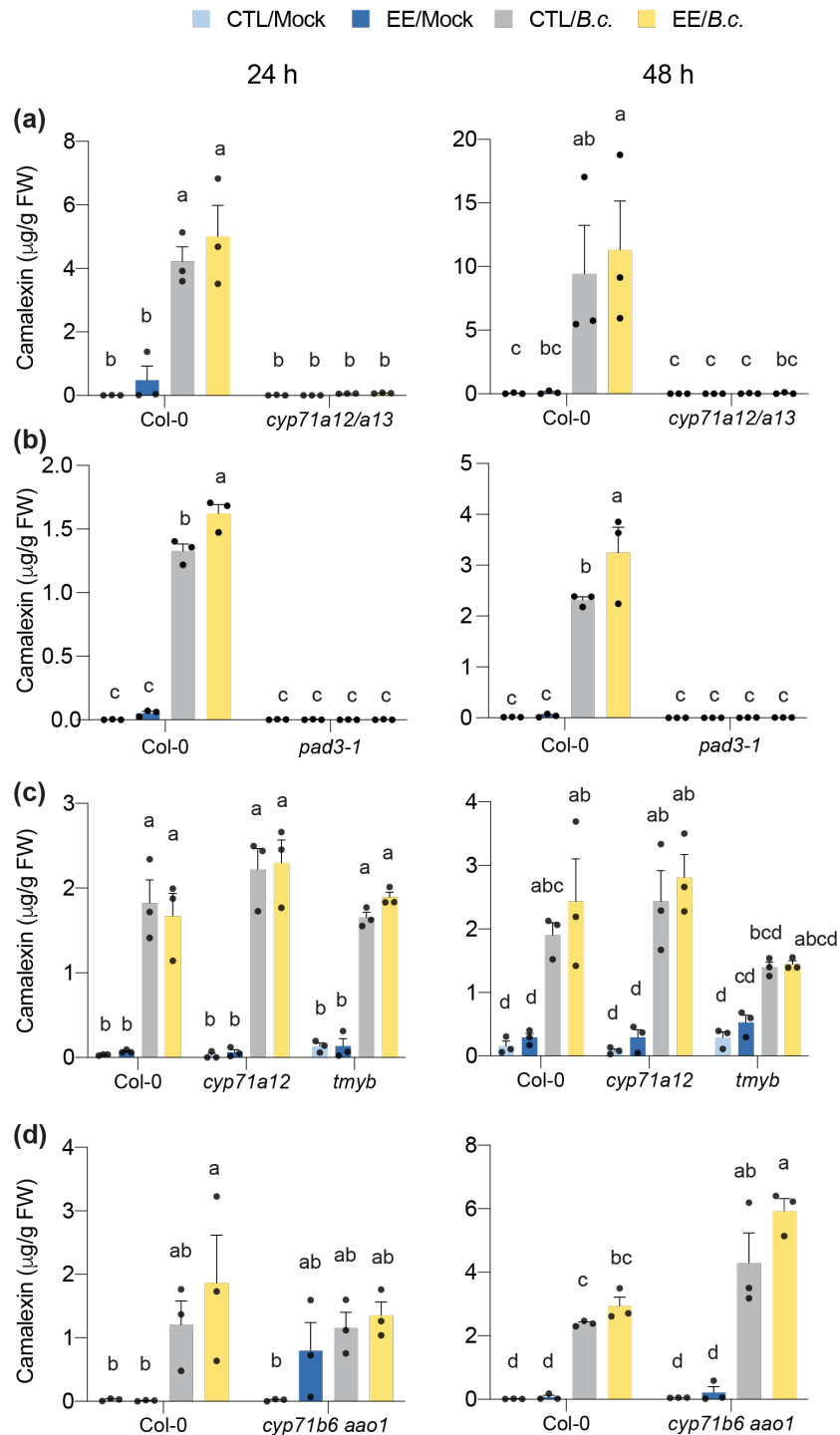


Fig. S10 Camalexin levels in various indolic mutants. (a-d) Levels of camalexin were quantified in distal leaves from 24 h and 48 h after *Botrytis cinerea* infection. Local leaves were pretreated with *Pieris brassicae* egg extract (EE) for 5 days or left untreated (CTL) and then distal leaves were infected with *B. cinerea* (*B.c.*) or a mock solution (Mock). Means \pm SE of three independent experiments are shown (n = 10-12 per experiment). Different letters indicate significant differences at $P < 0.05$ (ANOVA followed by Tukey's Honest Significant Difference test). *tmyb* = *myb34 myb51 myb122*.

Table S2 Time-course of single glucosinolate species accumulation.

Metabolite	Abb.	Col-0 12 h			
		CTL/Mock	EE/Mock	CTL/ <i>B.c.</i>	EE/ <i>B.c.</i>
Glucosinolate ¹	3MSOP	20.55 ± 4.33	25.25 ± 2.00	21.22 ± 3.20	26.41 ± 2.63
Glucoraphanin ¹	4MSOB	141.15 ± 33.5	173.7 ± 16.9	135.29 ± 30.2	175.69 ± 30.6
Glucosinolate ¹	5MSOP	4.76 ± 0.99	5.65 ± 0.64	4.29 ± 0.83	5.8 ± 0.95
Glucosinolate ¹	7MSOH	2.8 ± 0.77	3.18 ± 0.38	2.23 ± 0.33	3.3 ± 0.57
Glucosinolate ¹	4MTB	75.3 ± 8.89	86.91 ± 2.98	69.15 ± 13.3	79.34 ± 10.1
Glucobrassicin ²	I3M	32.05 ± 5.97	35.93 ± 4.73	34.47 ± 2.37	35.26 ± 1.64
Hydroxyglucobrassicin ²	OH-I3M	3.95 ± 0.64	4.47 ± 0.52	4.24 ± 0.32	4.53 ± 0.17
Methoxyglucobrassicin ²	4MOI3M	4.75 ± 0.44	6.57 ± 0.42	5.13 ± 0.35	6.7 ± 0.61
Neoglucobrassicin ²	1MOI3M	0.57 ± 0.06	0.69 ± 0.05	0.52 ± 0.05	0.66 ± 0.04
Col-0 24 h					
		CTL/Mock	EE/Mock	CTL/ <i>B.c.</i>	EE/ <i>B.c.</i>
Glucosinolate ¹	3MSOP	17.81 ± 2.38	23.29 ± 3.04	21.41 ± 3.47	28.38 ± 7.21
Glucoraphanin ¹	4MSOB	121.09 ± 13.3	126.85 ± 14.1	136.67 ± 19.6	199.84 ± 58.6
Glucosinolate ¹	5MSOP	4.12 ± 0.41	4.99 ± 0.66	4.58 ± 0.28	7.04 ± 1.39
Glucosinolate ¹	7MSOH	2.41 ± 0.25	2.77 ± 0.23	2.59 ± 0.19	4.34 ± 0.75
Glucosinolate ¹	4MTB	52.42 ± 6.00	63.03 ± 11.6	64.97 ± 5.63	91.19 ± 20.6
Glucobrassicin ²	I3M	26.02 ± 1.47	32.05 ± 2.81	28.5 ± 1.31	36.58 ± 5.25
Hydroxyglucobrassicin ²	OH-I3M	3.23 ± 0.26	4 ± 0.40	3.57 ± 0.16	4.82 ± 0.74
Methoxyglucobrassicin ²	4MOI3M	5.45 ± 0.73	6.61 ± 0.56	6.29 ± 0.33	8.95 ± 1.06
Neoglucobrassicin ²	1MOI3M	0.53 ± 0.10	0.61 ± 0.13	0.6 ± 0.02	0.79 ± 0.13
Col-0 48 h					
		CTL/Mock	EE/Mock	CTL/ <i>B.c.</i>	EE/ <i>B.c.</i>
Glucosinolate ¹	3MSOP	15.16 ± 2.25	19.87 ± 3.31	14.93 ± 2.86	15.09 ± 1.42
Glucoraphanin ¹	4MSOB	92.95 ± 15.1	126.81 ± 23.9	90.99 ± 14.5	90.08 ± 9.98
Glucosinolate ¹	5MSOP	3.42 ± 0.62	4.49 ± 0.60	3.32 ± 0.59	3.46 ± 0.32
Glucosinolate ¹	7MSOH	2.2 ± 0.33	2.77 ± 0.50	1.81 ± 0.31	2.05 ± 0.25
Glucosinolate ¹	4MTB	48.18 ± 6.95	67.64 ± 15.9	56.15 ± 16.5	51.3 ± 10.9
Glucobrassicin ²	I3M	19.18 ± 5.96	24.28 ± 3.94	14.82 ± 2.65	15.71 ± 3.02
Hydroxyglucobrassicin ²	OH-I3M	2.35 ± 0.68	3.13 ± 0.49	1.92 ± 0.35	2.13 ± 0.39
Methoxyglucobrassicin ²	4MOI3M	5.64 ± 0.63	6.76 ± 0.49	6.33 ± 0.86	7.1 ± 0.30
Neoglucobrassicin ²	1MOI3M	0.53 ± 0.13	0.66 ± 0.13	0.86 ± 0.10	1.18 ± 0.34

Levels of single aliphatic¹ and indole² glucosinolate species in µg/g FW, quantified in distal leaves from 12 h to 48 h after *Botrytis cinerea* (*B.c.*) infection or treatment with a mock solution (Mock) in Col-0, with or without pretreatment for 5 days with *Pieris brassicae* egg extract (EE). Means ± SE of three independent experiments are shown (n = 10-12 leaves per sample/experiment). Total aliphatic and indole glucosinolates are shown in Fig. S5a and c. Abb. = Abbreviation.

Table S3 Single glucosinolate species in Col-0 and *tmyb* mutant.

Metabolite	Abb.	Col-0							
		CTL/Mock		EE/Mock		CTL/ <i>B.c.</i>		EE/ <i>B.c.</i>	
Glucoiberin ¹	3MSOP	16.97	± 3.59	22.28	± 3.07	16.25	± 3.30	22.93	± 4.42
Glucoraphanin ¹	4MSOB	114.18	± 23.3	165.43	± 29.8	107.13	± 22.2	170.10	± 39.6
Glucoalyssin ¹	5MSOP	3.17	± 0.63	4.04	± 0.54	3.01	± 0.59	4.29	± 0.81
Glucoibarin ¹	7MSOH	1.32	± 0.54	1.71	± 0.40	1.08	± 0.37	1.66	± 0.52
Glucohirsutin ¹	8MSOO	16.17	± 4.98	20.78	± 3.87	12.89	± 3.62	19.86	± 3.59
Glucoerucin ¹	4MTB	40.12	± 7.84	56.9	± 11.9	36.08	± 8.08	52.58	± 14.4
Glucoberteroin ¹	5MTB	3.47	± 0.64	4.29	± 0.57	3.11	± 0.66	4.31	± 1.02
Gluconasturtiin ¹	2PE	0.64	± 0.18	0.88	± 0.24	0.59	± 0.16	0.85	± 0.29
7-Methylthioheptyl-GS ¹	7MTH	7.19	± 1.73	7.72	± 1.07	6.48	± 1.19	7.74	± 1.84
8-Methylthiooctyl-GS ¹	8MTO	24.91	± 5.31	27.68	± 2.78	20.27	± 3.21	26.51	± 4.74
Glucobrassicin ²	I3M	20.22	± 3.23	23.53	± 2.35	18.11	± 2.59	25.54	± 3.55
Hydroxyglucobrassicin ²	OH-I3M	2.3	± 0.40	2.85	± 0.35	2.32	± 0.42	3.38	± 0.74
Methoxyglucobrassicin ²	4MOI3M	4.62	± 0.58	4.88	± 0.61	3.37	± 0.27	4.3	± 0.33

<i>tmyb</i>									
	Abb.								
		CTL/Mock		EE/Mock		CTL/ <i>B.c.</i>		EE/ <i>B.c.</i>	
Glucoiberin ¹	3MSOP	25.40	± 4.21	25.64	± 1.9	23.01	± 3.80	24.47	± 4.54
Glucoraphanin ¹	4MSOB	169.51	± 40.4	170.85	± 6.9	150.64	± 31.8	158.51	± 32.5
Glucoalyssin ¹	5MSOP	4.58	± 0.55	4.42	± 0.6	4.13	± 0.62	4.38	± 0.81
Glucoibarin ¹	7MSOH	2.43	± 0.75	2.24	± 0.2	2.06	± 0.74	2.36	± 0.73
Glucohirsutin ¹	8MSOO	28.56	± 9.87	24.63	± 0.9	22.89	± 6.74	24.69	± 6.31
Glucoerucin ¹	4MTB	70.87	± 21.8	69.56	± 3.3	62.64	± 16.9	75.05	± 15.8
Glucoberteroin ¹	5MTB	4.92	± 0.66	5.08	± 0.4	4.3	± 0.57	4.86	± 0.78
Gluconasturtiin ¹	2PE	1.09	± 0.27	1.09	± 0.2	0.99	± 0.28	1.16	± 0.24
7-Methylthioheptyl-GS ¹	7MTH	10.91	± 1.12	9.94	± 1.7	9.37	± 1.34	10.2	± 2.18
8-Methylthiooctyl-GS ¹	8MTO	30.97	± 5.29	27.49	± 3.5	25.21	± 3.43	27.06	± 4.46
Glucobrassicin ²	I3M	n.d.		n.d.		n.d.		n.d.	
Hydroxyglucobrassicin ²	OH-I3M	n.d.		n.d.		n.d.		n.d.	
Methoxyglucobrassicin ²	4MOI3M	n.d.		n.d.		n.d.		n.d.	

Levels of single aliphatic¹ and indole² glucosinolate species in µg/g FW, quantified in distal leaves 24 h after *Botrytis cinerea* infection or treatment with a mock solution (Mock) in Col-0 and *tmyb*, with or without pretreatment for 5 days with *Pieris brassicae* egg extract (EE). Means ± SE of three independent experiments are shown (n = 10-12 leaves per sample/experiment). Total aliphatic and indole glucosinolates are shown in Fig. S5b and d. Abb. = Abbreviation, n.d. = not detectable. *tmyb* = *myb34 myb51 myb122*.

Methods S1 Lines used in this study.

Lines used in this study: *ald1* (Návarová *et al.*, 2012), *cyp71a12* (Millet *et al.*, 2010), *cyp71a12 cyp71a13* (Müller *et al.*, 2015), *cyp79b2 cyp79b3* (Zhao *et al.*, 2002), *cyp82c2-2* (Rajniak *et al.*, 2015), *fmo1* (Mishina & Zeier, 2006), *fox1* (Rajniak *et al.*, 2015), *ics1* (Nawrath & Métraux, 1999), *ics2* (Garcion *et al.*, 2008), *lecrk-1.8* (Gouhier-Darimont *et al.*, 2013), *myb28 myb29* (Beekwilder *et al.*, 2008), *myb34 myb51 myb122 (tmyb)* (Frerigmann & Gigolashvili, 2014), *nahG* (Nawrath & Métraux, 1999), *npr1-1* (Cao *et al.*, 1997), *npr1-1 npr4-4D* (Liu *et al.*, 2020), *pad3-1* (Glazebrook & Ausubel, 1994), *wrky33* (Birkenbihl *et al.*, 2012). All genotypes were in the Columbia (Col-0) background. The *cyp71b6 aao1* double mutant was obtained by crossing single mutants described previously, *cyp71b6* (GABI_305A04) and *aao1* (SALK_069221) (Müller *et al.*, 2019). Genotyping was done using the following primers: CYP71B6 (At2g24180) LP: 5'-CCAGGTGCTTCTTCAACACTC-3', RP: 5'-TCATCTGGATCTTCCGTTGAC-3'; AAO1 (At5g20960) LP: 5'-AGCAGCTCGAGTCAAGAACAG-3', RP: 5'-TGCAATATCTGCATGCTTTTG-3'. The *ics1^{-/-} ics2^{+/-}* double mutant (homozygous for *ics1*, heterozygous for *ics2*) was obtained by crossing *ics1* and *ics2*, and was genotyped using a CAPS marker for *ics1* (Heck *et al.*, 2003) and flanking primers for *ics2* T-DNA knockout (Garcion *et al.*, 2008). *ICS1* (At1g74710) Fw: 5'-GGA CTC AAT TAG GTG TCT GC-3', Rv: 5'-AAG CCT TGC TTC TTC TGC TG-3'; *ICS2* (At1g18870) Fw: 5'-GTC TTC AAA GTC TCC TCT GAT-3' Rv: 5'-TGA ATC ACC TCT AGG CCT TGT-3'.

Methods S2 Measurement of *Botrytis cinerea* growth by QPCR.

Total RNA from a pool of 10-12 leaves was extracted using a ReliaPrep™ RNA Tissue Miniprep System (Promega). For cDNA synthesis, 500 ng of total RNA was reverse-transcribed using M-MLV reverse transcriptase (Invitrogen) in a final volume of 15.25 µl. Each cDNA sample was generated in triplicate and diluted eightfold with water. Quantitative real-time PCR analysis was performed in a final volume of 20 µl containing 2 µl of cDNA, 0.2 µM of each primer, 0.03 µM of reference dye and 10 µl of Brilliant III Ultra Fast SYBR Green qPCR Master Mix (Agilent). Reactions were performed using an Mx3000P real-time PCR machine (Agilent) with the following program: 95°C for 3 min, then 40 cycles of 10 sec at 95°C and 20 sec at 60°C. Relative mRNA abundance of *Bc Tubulin* was normalized to the housekeeping gene *PUX1* (Windram *et al.*, 2012). The following primers were used: *Bc Tub* (Broad MIT ID: BC1G_00122) Fw: 5'-

TTCCATGAAGGAGGTTGAGG-3', Rv: 5'-TACCAACGAAGGTGGAGGAC-3'; PUX1
(At3g27310) Fw: 5'-AATGTTGCCTCCAATGTGTGA-3', Rv: 5'-
TTTTTACCGCCTTTTGGCTAC-3'.

Methods S3 Metabolite analyses.

For metabolite analyses, an Acquity UPLC system coupled to a Synapt G2 QTOF mass spectrometer (Waters, Milford, MA) was employed. The entire system was controlled by Masslynx 4.1. The separation was performed in gradient mode on an Acquity BEH C18 column, 50 x 2.1 mm, 1.7 μ m particle size (Waters) using a flow rate of 0.4 mL/min and mobile phases consisting of H₂O + formic acid 0.05% (phase A) and acetonitrile + formic acid 0.05% (phase B). The gradient program started at 2% B, increased linearly to 60% B in 4.0 min, then to 100% B in 2.0 min, the column was then washed with 100% B for 2.0 min before re-equilibration at initial conditions (2% B) for 2.0 min. The column temperature was maintained at 25°C throughout the run. The injection volume was 2 μ L (partial loop with needle overfill mode). Mass spectrometric detection was performed in electrospray negative mode using a mass range of 50-600 Da. The MS capillary voltage was -2.0 kV, the cone voltage was -25V, the desolvation temperature and gas flow were 500°C and 800 L/h, respectively, the cone gas flow was 20 L/h, and the detector voltage was 2250 V. Accurate mass measurements were provided by infusing a 500 ng/mL solution of leucine-enkephalin through the LockSpray probe at a flow rate of 15 μ L/min. The quantification of ICA was achieved by external calibration using calibration points at 5, 20, 100, 500 and 2000 ng/mL.

For analysis of leaf surface camalexin, *Botrytis cinerea*-infected or mock-treated leaves were immersed in 80% MeOH (2 mL/ 2 leaves) in 6-well plates and gently rotated for 30 sec. The solvent was collected in Eppendorf tubes and evaporated using a speed vac. The pellet was resuspended in 200 μ l of 80% MeOH and transferred to vials for further LC-MS analysis. Quantification of camalexin was done according to (Balmer *et al.*, 2018). Values were normalized to the leaf surface and expressed as μ g/cm². A total of 8 leaves (2 leaves from 4 plants) was used for each biological replicate.

References

- Balmer A, Pastor V, Glauser G, Mauch-Mani B. 2018.** Tricarboxylates Induce Defense Priming Against Bacteria in *Arabidopsis thaliana*. *Frontiers in Plant Science* **9**: 1221.
- Beekwilder J, van Leeuwen W, van Dam NM, Bertossi M, Grandi V, Mizzi L, Soloviev M, Szabados L, Molthoff JW, Schipper B, et al. 2008.** The impact of the absence of aliphatic glucosinolates on insect herbivory in *Arabidopsis*. *PLoS one* **3**: e2068.
- Birkenbihl RP, Diezel C, Somssich IE. 2012.** *Arabidopsis* WRKY33 is a key transcriptional regulator of hormonal and metabolic responses toward *Botrytis cinerea* infection. *Plant Physiology* **159**: 266–285.
- Cao H, Glazebrook J, Clarke JD, Volko S, Dong X. 1997.** The *Arabidopsis* NPR1 gene that controls systemic acquired resistance encodes a novel protein containing ankyrin repeats. *Cell* **88**: 57–63.
- Frerigmann H, Gigolashvili T. 2014.** MYB34, MYB51, and MYB122 distinctly regulate indolic glucosinolate biosynthesis in *Arabidopsis thaliana*. *Molecular Plant* **7**: 814–828.
- Garcion C, Lohmann A, Lamodièrre E, Catinot J, Buchala A, Doermann P, Mettraux J-P. 2008.** Characterization and biological function of the ISOCHORISMATE SYNTHASE2 gene of *Arabidopsis*. *Plant Physiology* **147**: 1279–1287.
- Glazebrook J, Ausubel FM. 1994.** Isolation of phytoalexin-deficient mutants of *Arabidopsis thaliana* and characterization of their interactions with bacterial pathogens. *Proceedings of the National Academy of Sciences, USA* **91**: 8955–8959.
- Gouhier-Darimont C, Schmiesing A, Bonnet C, Lassueur S, Reymond P. 2013.** Signalling of *Arabidopsis thaliana* response to *Pieris brassicae* eggs shares similarities with PAMP-triggered immunity. *Journal of Experimental Botany* **64**: 665–674.
- Heck S, Grau T, Buchala A, Mettraux J-P, Nawrath C. 2003.** Genetic evidence that expression of NahG modifies defence pathways independent of salicylic acid biosynthesis in the *Arabidopsis*-*Pseudomonas syringae* pv. tomato interaction. *Plant Journal* **36**: 342–352.
- Liu Y, Sun T, Sun Y, Zhang Y, Radojic A, Huang X, Lan J, Chen S, Orduna AR, Zhang K, et al. 2020.** Diverse Roles of the Salicylic Acid Receptors NPR1 and NPR3/NPR4 in Plant Immunity. *Plant Cell* **32**: 4002–4016.
- Millet YA, Danna CH, Clay NK, Songnuan W, Simon MD, Werck-Reichhart D, Ausubel FM. 2010.** Innate immune responses activated in *Arabidopsis* roots by microbe-associated molecular patterns. *Plant Cell* **22**: 973–990.
- Mishina TE, Zeier J. 2006.** The *Arabidopsis* flavin-dependent monooxygenase FMO1 is an essential component of biologically induced systemic acquired resistance. *Plant Physiology* **141**: 1666–1675.

Müller TM, Böttcher C, Glawischnig E. 2019. Dissection of the network of indolic defence compounds in *Arabidopsis thaliana* by multiple mutant analysis. *Phytochemistry* **161**: 11–20.

Müller TM, Böttcher C, Morbitzer R, Götz CC, Lehmann J, Lahaye T, Glawischnig E. 2015. TRANSCRIPTION ACTIVATOR-LIKE EFFECTOR NUCLEASE-Mediated Generation and Metabolic Analysis of Camalexin-Deficient *cyp71a12 cyp71a13* Double Knockout Lines. *Plant Physiology* **168**: 849–858.

Návarová H, Bernsdorff F, Döring A-C, Zeier J. 2012. Pipecolic acid, an endogenous mediator of defense amplification and priming, is a critical regulator of inducible plant immunity. *Plant Cell* **24**: 5123–5141.

Nawrath C, Métraux JP. 1999. Salicylic acid induction-deficient mutants of *Arabidopsis* express PR-2 and PR-5 and accumulate high levels of camalexin after pathogen inoculation. *Plant Cell* **11**: 1393–1404.

Rajniak J, Barco B, Clay NK, Sattely ES. 2015. A new cyanogenic metabolite in *Arabidopsis* required for inducible pathogen defence. *Nature* **525**: 376–379.

Windram O, Madhou P, McHattie S, Hill C, Hickman R, Cooke E, Jenkins DJ, Penfold CA, Baxter L, Breeze E, et al. 2012. *Arabidopsis* defense against *Botrytis cinerea*: chronology and regulation deciphered by high-resolution temporal transcriptomic analysis. *Plant Cell* **24**: 3530–3557.

Zhao Y, Hull AK, Gupta NR, Goss KA, Alonso JM, Ecker JR, Normanly J, Chory J, Celenza JL. 2002. Trp-dependent auxin biosynthesis in *Arabidopsis*: involvement of cytochrome P450s CYP79B2 and CYP79B3. *Genes & Development* **16**: 3100–3112.